Photovoltaic Systems Modeling and Analysis

BY

MIR SHAHED ALI

A Thesis Presented to the

DEANSHIP OF GRADUATE STUDIES

KING FAHD UNIVERSITY OF PETROLEUM & MINERALS

DHAHRAN, SAUDI ARABIA

In Partial Fulfillment of the
Requirements for the Degree of

MASTER OF SCIENCE

In

ELECTRICAL ENGINEERING

DECEMBER 2010

i

KING FAHD UNIVERSITY OF PETROLEUM AND MINERALS

DHAHRAN 31261, SAUDI ARABIA

DEANSHIP OF GRADUATE STUDIES

This thesis, written by Mir Shahed Ali under the direction of his thesis advisor and approved by his thesis committee, has been presented to and accepted by the Dean of Graduate Studies, in partial fulfillment of the requirements for the degree of **MASTER OF SCIENCE IN ELECTRICAL ENGINEERING.**

Thesis Committee

Dr. Ibrahim M El-Amin (Advisor)

Dr. A. H. Abdurrahim (Member)

Dr. Mohammad Ali Y Abido (Member)

Dr. S. H. Abdul-Jauwad

Department Chairman

Dr. Salam A. Zummo

Dean of Graduate Studies

9/1/11

Date

i

Dedicated to

My Parents, Sisters

And

Teachers

ACKNOWLEDGEMENTS

In the name of Allah, the most Merciful, the most Gracious. All praise is due to Allah; we praise Him, seek His help, and ask for forgiveness. Peace be upon the Prophet Mohammad, his family, his companions, and all those who followed him until the Day of Judgment.

I am greatly indebted to my thesis advisor Dr. Ibrahim M El-Amin for his constant support, encouragement and guidance in successfully accomplishing this work. I am grateful to his time, patience and in valuable suggestions that he gave during the course of thesis work. I would like to express my deepest appreciation towards him.

I would also express my grateful thanks to my thesis committee members, Dr. A. H. Abdurrahim and Dr. Mohammad Ali Y Abido for their cooperation and involvement and the time they spared to review this thesis. Special thanks also to Dr. S. H. Abdul-Jauwad, Chairman of EE department and the King Fahd University of Petroleum & Minerals for providing an opportunity and excellent facilities of research.

I am very thankful to my parents, sisters and brother-in-law for their constant support, love, patience and prayers without which I would not be able to accomplish such a great task. Their commitment, enthusiasm and encouragement have always been the source of motivation for my goals.

I would also like to thank all my colleagues, friends and seniors at KFUPM for providing the moral support and a pleasant atmosphere which helped me overcome the very thought of being away from home.

TABLE OF CONTENTS

ACKNOWLEDGEMENTS iii
TABLE OF CONTENTS iv
LIST OF TABLES vii
LIST OF FIGURES viii
THESIS ABSTRACT (ENGLISH) xii
THESIS ABSTRACT (ARABIC) xiii
Nomenclature xiv

Chapter 1 1

1. Introduction 1

1.1. Overview 1
1.2. Development of Photovoltaic System 4
1.3. Thesis Motivation 6
1.4. Thesis Objective 7
1.5. Thesis Organization 8

CHAPTER 2 9

2. Literature Survey 9

2.1. The physics behind PV modules 9
2.2. Band Structure and Band Gap Energy 10
2.3. Doping 14
2.4. The p-n junction 15
2.5. Types of Photovoltaic Cells 17
2.6. Advantages of Photovoltaic 19
2.7. Disadvantages of Photovoltaic's 20
2.8. Building of Large PV Arrays 21
2.9. Boosting Voltage and Amperage 22
2.10. Worldwide Installation of PV 22
2.11. Problems associated with PV Arrays 24

2.12. Problems due to the integration of Photovoltaic Generators with the power system 24

CHAPTER 3 33

3. System Modeling.....33

3.1. System Description 33
3.2. The Photovoltaic Cell 34
3.3. The Photovoltaic Module..... 42
3.3.1. Bypass diode: 45
3.3.2. Isolation/Blocking Diodes:..... 45
3.4. The Photovoltaic Array..... 46
3.4.1. Determination of PV Module Parameters 49
3.5. The Power Conditioning Unit..... 50
3.5.1. DC/DC Converter..... 51
3.5.1.1. Buck Converter Topology 52
3.5.1.2. Theory of Operation 53
3.5.1.3. Sizing the output filter 56
3.5.2. Maximum Power Point Tracking 60
3.5.2.1. Maximum Power Point Method 61
3.6. Battery..... 62
3.7. The DC to AC Inverter 63

CHAPTER 4 72

4. Results and Discussion 72

4.1. PV cluster system steady-state simulation..... 84
4.2. PV cluster system fault analysis 87
4.3. Fault analysis due to the fault occurred at the secondary of the transformer T3 of the PV generator or at the inverter output terminal 97

CHAPTER 5 103

5. Conclusion 103

5.1. Future Work 105
6. References 106
Vita 113

LIST OF TABLES

Table 2-1: The list of the major PV power stations in the world is given in the following table. 23

Table 3-1: Transformer data summary 69

Table 3-2: Line impedance summary 69

Table 3-3: Load data Summary 70

Table 4-1: Change in voltage levels (pu) of seven busses for different levels of PV penetration 85

LIST OF FIGURES

Figure 2-1: The solar spectrum at AM1.5 13

Figure 2-2: The p-n junction.....16

Figure 3-1: Ideal I-V curve for PV cell. 35

Figure 3-2: Typical I-V characteristic curve of a PV cell 35

Figure 3-3: Electrical equivalent model of Solar Cell.....38

Figure 3-4: Appropriate Model.....41

Figure 3-5: General Model of PV Module 42

Figure 3-6: String of cells with bypass and blocking diodes 44

Figure 3-7: General Model of PV Module 48

Figure 3-8: Appropriate Model of PV Module 49

Figure 3-9: Components of the power conditioning unit 51

Figure 3-10: Electrical Model - DC/DC converter (Buck topology) 53

Figure 3-11: Switch Operation – DC/DC Converter.....54

Figure 3-12: Inductor Current Waveform – Output Filter 57

Figure 3-13: Inductor Current Waveforms used to Illustrate Capacitor Charging.....59

Figure 3-14: Simulink block diagram of the PV generator integrated with Utility System 65

Figure 3-15: PV generator sub-system 66

Figure 3-16: MPPT block sub-system 67

Figure 3-17: Determination of open circuit voltage subsystem 68

Figure 3-18: Single Line Diagram of solar charger 71

Figure 4-1: V-I Characteristics at different values of solar irradiance.....73

Figure 4-2: P-V Characteristics at different values of solar irradiance G=1=1000W/m2. 74

Figure 4-3: I-V Characteristics at different values of cell's temperature.....75

Figure 4-4: P-V Characteristics at different values of cell's temperature.....76

Figure 4-5: Single Line Diagram of Solar Charger 77

Figure 4-6: I-V Characteristics of a PV array generating 32KW power at different values of solar irradiance 79

Figure 4-7: P-V Characteristics of a PV array generating 32KW power at different values of solar irradiance. 80

Figure 4-8: I-V Characteristics of a PV array generating 32KW power at different values cell's temperature. 81

Figure 4-9: P-V Characteristics of a PV array generating 32KW power at different values cell's temperature. 82

Figure 4-10: Inverter output voltage.....83

Figure 4-11: Transformer output voltage 83

Figure 4-12: Voltage profile of bus 7 with 32KW of PV generator integrated at bus 7 86

Figure 4-13: RMS voltage profile of bus 7 with 32KW of PV generator integrated at bus 7.....86

Figure 4-14: Voltage profile of bus 7 if a three phase fault occurred at bus 5 with 32KW PV generator connected at bus 7. 87

Figure 4-15: RMS value of the voltage at bus 7 if a three phase fault occurred at bus 5 with 32KW PV generator connected at bus 7.....88

Figure 4-16: Voltage profile of bus 5 if a three phase fault occurred at bus 5 with 32KW PV generator connected at bus 7. 89

Figure 4-17: Voltage profile of bus 4 if a three phase fault occurred at bus 5 with 32KW PV generator connected at bus 7. 90

Figure 4-18: Voltage profile of bus 3 if a three phase fault occurred at bus 5 with 32KW PV generator connected at bus 7. 90

Figure 4-19: Voltage profile of bus 2 if a three phase fault occurred at bus 5 with 32KW PV generator connected at bus 7. 91

Figure 4-20: Voltage profile of bus 1 if a three phase fault occurred at bus 5 with 32KW PV generator connected at bus 7. 91

Figure 4-21: Voltage profile of bus 7 if a single phase fault occurred at bus 7 with 32KW PV generator connected to bus 7. 92

Figure 4-22: RMS value of the voltage at bus 7 if a single phase fault occurred at bus 7 with 32KW PV generator connected at bus 7.....93

Figure 4-23: Voltage profile of bus 5 if a single phase fault occurred at bus 7 with 32KW PV generator connected to bus 7. 94

Figure 4-24: Voltage profile of bus 4 if a single phase fault occurred at bus 7 with 32KW PV generator connected to bus 7. 94

Figure 4-25: Voltage profile of bus 3 if a single phase fault occurred at bus 7 with 32KW PV generator connected to bus 7. 95

Figure 4-26: Voltage profile of bus 2 if a single phase fault occurred at bus 7 with 32KW PV generator connected to bus 7. 95

Figure 4-27: Voltage profile of bus 1 if a single phase fault occurred at bus 7 with 32KW PV generator connected to bus 7. 96

Figure 4-28: Voltage profile of bus 7 if a single phase fault occurred at the secondary of the transformer T3 with 32KW PV generator connected to bus 7. 97

Figure 4-29: Voltage profile of bus 5 if a single phase fault occurred at the secondary of the transformer T3 with 32KW PV generator connected to bus 7. 98

Figure 4-30: Voltage profile of bus 4 if a single phase fault occurred at the secondary of the transformer T3 with 32KW PV generator connected to bus 7. 99

Figure 4-31: Voltage profile of bus 3 if a single phase fault occurred at the secondary of the transformer T3 with 32KW PV generator connected to bus 7. 99

Figure 4-32: Voltage profile of bus 2 if a single phase fault occurred at the secondary of the transformer T3 with 32KW PV generator connected to bus 7. 100

Figure 4-33: Voltage profile of bus 1 if a single phase fault occurred at the secondary of the transformer T3 with 32KW PV generator connected to bus 7. 100

Figure 4-34: Voltage profile of inverter output if a single phase fault occurred at the secondary of the transformer T3 with 32KW PV generator connected to bus 7. 101

Figure 4-35: The ‘state of charge’ of the battery if a single phase fault occurs at the secondary of the transformer T3 with 32KW PV generator connected to bus 7.....101

THESIS ABSTRACT (ENGLISH)

NAME: MIR SHAHED ALI
TITLE: Photovoltaic Systems Modeling and Analysis
MAJOR: ELECTRICAL ENGINEERING
DATE: DECEMBER 2010

This thesis deals with the implementation of generalized photovoltaic model and integration of the same with 7-bus electrical utility system to evaluate the impact that the photovoltaic generator have on the utility system. Among all the impacts that the photovoltaic generator have on the utility system, voltage rise of the power distribution line at the position where the Photovoltaic generator is connected due to reverse power flow from the photovoltaic model has been one of the major problem. Therefore, this thesis proposes the steady-state simulations to evaluate the effectiveness of battery-integrated PV system on avoiding the over voltage problem. Further, fault analysis is done to study the effect of the PV model on the utility network during faults and it is deduced that the impact of the PV model on the utility system voltage during faults is nominal. The photovoltaic model/generator and the 7-bus utility system is developed using Matlab/Simulink software package. The developed photovoltaic model can be represented as PV cell, module or an array [11]. The model is developed with icons that are easy to understand. The developed model takes into consideration cell's working temperature, amount of sunlight (irradiance) available, voltage of the circuit when the circuit is open and current of the circuit when it is shorted. The developed Photovoltaic model is then integrated with a Li-ion battery, over here battery serves two purposes first it will store the excess power from the Photovoltaic generator if any, during the day time and in night the battery acts as an generator and deliver the power to the utility or connected load with the help of an invertors.

MASTER OF SCIENCE DEGREE
KING FAHD UNIVERSITY OF PETROLEUM and MINERALS
Dhahran, Saudi Arabia

THESIS ABSTRACT (ARABIC)

الاسم : علي الشهيد مير

العنوان : الضوئية نظم النمذجة والتحليل

التخصص : هندسة كهربائية

التاريخ : ديسمبر 2010

تتناول هذه الرسالة مع تنفيذ نموذج معمم الضوئية والتكامل في نفس الحافلة - 7 مع أنظمة كهربائية للفائدة لتقييم الأثر الذي مولد الضوئية وعلى النظام فائدة. بين الآثار جميعا أن مولد الضوئية وعلى النظام فائدة ، وارتفاع الجهد من قوة خط التوزيع في نقطة اقتران المشتركة (العصابة) نتيجة لتدفق الطاقة من طراز عكس الضوئية كان واحدا من المشكلة الرئيسية. لذلك ، هذه الرسالة تقترح محاكاة حالة ثابتة لتقييم فعالية النظام الكهروضوئية بطارية متكاملة على تجنب ما يزيد على مشكلة التيار الكهربائي. كذلك ، يتم تحليل خطأ لتحليل تأثير النموذج الضوئية على النظام خلال الأداة أخطاء ووجد أن تأثير نموذج الضوئية على فائدة الجهد خلال نظام أخطاء غير الاسمية. تم تطوير نموذج الضوئية / مولد ونظام فائدة 7 - حافلة باستخدام برنامج ماتلاب Simulink / الحزمة. يمكن تمثيل النموذج المطور الضوئية والخلايا الكهروضوئية ، وحدة أو مجموعة لسهولة استخدامها على منصة المحاكاة. تم تطوير النموذج المقترح مع رموز سهلة الاستعمال ، وهذا يجعل من نموذج محاكاة الكهروضوئية المعمم بسهولة وتحليلها بالتعاون مع الالكترونيات السلطة لتعقب باور بوينت الأقصى. نموذج المتقدمة يأخذ في الاعتبار درجة الحرارة خلية عمل ، كمية ضوء الشمس (الإشعاعية) المتاحة ، والجهد الدائرة المفتوحة وماس كهربائى الحالي. ثم تم دمج النموذج المطور الضوئية مع بطارية ليثيوم أيون ، أكثر من هنا البطارية يخدم غرضين لأول مرة سيتم تخزين الطاقة الزائدة من المولدات الكهربائية الضوئية إن وجدت ، خلال النهار والليل في البطارية بمثابة مولد وتسليم السلطة للفائدة أو تحميل مرتبطة مساعدة منsrotrevnI.

شهادة ماجستير علوم

جامعة الملك فهد للبترول والمعادن

الظهران ، المملكة العربية السعودية

Nomenclature

j	Joules
σ	Stefan-Boltzmann constant
T	Temperature in Kelvin
h	Plank's constant
c	Speed of light
k	Boltzmann constant
ג	Wavelength in meters.
SC	Solar constant
n	number of the day
W	watt
m	Meter
β	Altitude angle of the sun
Θ	Angle of incidence
∑	Tilt angle of the collector
ṕ	Uniform reflection
ev	Electron volt
MW	Megawatts
ϕ	Phase

R	Resistance
L	Inductance
V	Voltage
P	Power
I	Current
f	Frequency
I_{SC}	Current of the circuit when it is shorted
V_{OC}	Voltage of the circuit when it is open
I_{ph}	Source or photon current
i_D	Diode current
m	Ideal factor
V_T	Thermal potential
q	Electric charge of an electron
R_{sh}	Shunt resistance
I_S	Cell's saturation current in dark
K_1	Cell's temperature coefficient when the circuit is shorted
$T_{ref.}$	Reference temperature of the cell
ג	Irradiance or insolation of the Sun
I_{RS}	Reverse saturation current of the cell
E_G	Band-gap energy of semiconductor used

N_P Number of arrays in parallel

N_S Number of arrays in series

δ Duty cycle

i_L Inductor Current

v_L Voltage across inductor

M_V Voltage factor

E Internal voltage

E_0 Battery capacity, Ampere-hour (Ah)

B Exponential capacity, (Ah^{-1})

P_m Mechanical power

V_f Field Voltage

ω_{ref} Reference Speed (radian/second)

Chapter 1

1.Introduction

1.1.Overview

Tremendous increases of PV system installations have been experienced in Japan, Germany, and other countries. According to market studies conducted by the European PV industry association (EPIA), the fastest growing PV market is for grid connected systems instead of standalone systems. Some of the major obstacles for the introduction of PV in large scale are the soaring initial costs, the offered formation of the energy markets, the nature of solar resource (intermittent and low capacity factor), and lack of net metering and new electricity storage technologies for photovoltaic use [1].

The efficiency of a typical flat-plate PV module is defined as the ability of a module to convert solar energy into electrical energy. But still it is relatively low: laboratory experiments show the efficiency of 25% [2], but in commercial use the efficiencies reach only 14-17%. Nevertheless, considering the enormous amount of energy coming from the Sun, the potential of PV technology in electricity production is still remarkable.

Integration of PV with the grid introduced many technical issues such as voltage variations, harmonic distortions, reactive power requirements, earthing, lightning

protection, long term cycling of batteries, and the optimization of system controls. The major system impacts in cluster PV systems include voltage variations and unbalance, current and voltage harmonics, increase on short circuit capacity, grid islanding protection, and other power quality issues, such as flicker and stress on distribution transformer.

In clustered Photovoltaic structures, many of residential Photovoltaic systems are intensively mounted and grid-connected in the small urban area's power distribution network. Actually, there is no unique definition of a clustered PV system. In general, if the density of PV installations in an area or community is high, the system can be called as the cluster PV system. In the PV systems, voltage at the power distribution line will rise because of the reverse power flow from each PV system in clear days, especially for the connection of a bulky Photovoltaic model. But from the studies conducted on the demonstration sites it is clear that a restricted amount of cluster Photovoltaic generators in the world had major sum of output energy losses in some meticulous days [1], the increasing penetration of cluster PV generation would bring serious voltage rise problems in the future. Different solutions are available to mitigate the over voltage problem that are caused due to the integration of Photovoltaic models. However, they would cause energy losses because PV integrate control systems would need to regulate or stop outputting the power to the grid as the voltage reaches to the upper limit. In order to avoid this energy loss, the concept of battery integrated PV systems has been proposed in the world; it is generally to charge the battery during the daytime and use that stored energy during the night.

In this work, the equivalent component models in the battery integrated PV system including PV cell, maximum PV power output controller, battery charger and discharger, and DC/AC inverter have been built. The actual product specifications are adopted as the parameters of the component models. These practical models are very useful to system analyses.

Furthermore, a real distribution system was chosen as the PV cluster demonstration site because it consists of the largest PV capacity in Taiwan residence until now. The data of voltage, current and power were determined at the cluster PV system output terminals. Next, the fault analysis is done on this real PV system. The main aim of the fault analysis is to analyze the consequence of the faults at diverse busses on the voltage of the load bus. Through the fault analysis, the transient current, voltage, and power at each point of the Photovoltaic system can be observed.

The steady-state simulation by using power flow calculation has been performed in this research. Its purpose is to clarify the impact at the point of common coupling (PCC) like over-voltage problem due to integration of the PV generator of varying capacity. The main contribution of this work is to address the PV modeling of short-time transients and performance, and long-term impact on the distribution network by using an actual PV demonstration site in Taiwan.

1.2.Development of Photovoltaic System

The physical phenomena of converting light to electricity known as the photovoltaic (PV) effect was foremost witnessed in 1839 by Edmond Becquerel. Becquerel found that a voltage developed when an electrode of the two indistinguishable electrodes in a pathetic conducting solution was illuminated. The PV effect was first studied in solids, such as selenium, in the 1870s. Then selenium PV cells were first developed in the year 1880, they exhibited 1-2% efficiency in converting light to electricity. Selenium converts light in the visible part of the sun's spectrum; for this reason, it was quickly adopted by the emerging field of that time that is photometric which means light measuring devices. Even today light-sensitive cells on cameras for adjusting shutter speed to match illumination are made of selenium.

But the drawback of the selenium cells is that their cost is very high relative to the amount of power they produce at the efficiency of 1%. Meanwhile, research was carried out in the physics of PV phenomena. In 1920s and 1930s, major breakthrough was achieved in quantum mechanics that lead to the development of the Photovoltaic theory. In 1940s and early 1950s a major step forward in solar-cell technology came when a method was developed for producing highly pure crystalline silicon, this method is known as the Czochralski method. In 1954, a silicon photovoltaic cell with 4% efficiency was developed in Bell Telephone Laboratories, which they soon improved to 6% first and then 17% efficiency.

Today, photovoltaic systems are capable of converting one kilowatt of solar energy falling on one square meter into about hundred watts of electricity. One-hundred watts of electrical energy is enough to power most household appliances. In fact, standard solar cells covering the sun-facing roof space of a typical home can provide about 8500-Kilowatt-hours of electricity annually, which is about the average household's yearly electric consumption.

There are certain factors that make capturing of solar energy difficult. These factors are sun's low illuminating power per square meter; sunlight is intermittent, affected by time of day, climate, pollution, and season. Power sources which involve Photovoltaic's require either back-up from other sources or storage devices when the sun is obscured. Further, the investment expenditure of a photovoltaic arrangement is very high.

1.3. Thesis Motivation

Due to large integration of Photovoltaic generators to the grid, number of problems came up like, rise in voltage levels at the point of common coupling (PCC), introduction of harmonics into the system because of large usage of inverter to convert DC power to AC. Short-circuit capacity has increased to a great extent, and flickers are observed on the voltage waveforms.

Thus, analyzing the impact of Photovoltaic Generators on the stability of electrical power system and suggestion of solution will add great value to the field of research in Photovoltaic Generation. It will validate the advantage that Photovoltaic Generation has on the stability and it will prove one technology of the Photovoltaic Generation to be a good candidate for green electrical power generation.

1.4.Thesis Objective

The specific objectives of this work are as follows:

- Development of Standalone Photovoltaic model (generator) which takes into consideration solar insolation (irradiance) and cell temperature.
- Integration of the model with the power system and simulating the system to examine the impact of the photovoltaic generator on the arrangement.
- Study of the system performance under various operation scenarios like by increasing the capacity of the DG.
- Study the fault analysis of the system by applying single or three phase faults at different busses.

1.5. Thesis Organization

Chapter 2 describe the various techniques used in order to develop PV generator model, and various studies conducted to analyze the impact of the grid-connected PV generator at the point of common coupling like voltage rise, flickers, harmonics and coordination of protective devices.

Chapter 3 deals with description of model to be develop; this chapter gives brief idea about the functions performed by each sub-system, which helps in basic understanding of the whole model.

In chapter 4 system modeling is introduced, where we show in detail mathematical steps needed to develop the PV generator, Maximum Power Point Tracker (MPPT) and DC/DC converter. In this chapter the task performed by the battery, inverter in this work are described. Then the modeling of the distribution network is considered which consist of seven busses and it is fed from an utility system.

Chapter 5 deals with discussion of the results obtained from the analysis, like the limit for the capacity of the grid connected PV system, voltage rise issue is discussed, and the results of the analysis are shown and discussed.

CHAPTER 2

2.Literature Survey

2.1.The physics behind PV modules

Basically, the operation of photovoltaic (PV) cells is based on the photoelectric effect. The photoelectric effect is the emission of the electrons from the surface of a material (usually a metal) when light strikes the surface. The number of escaped electrons are mainly depended on the number of photons, i.e., the intensity of light, and energy of the electrons depends on the energy of the photons. [5]

The photoelectric effect for the generation of electricity is possible only when there is a voltage difference, thus the electron is liberated – and this is where solid state technology enters the picture. The means for moving the mobile electrons in the desired manner are provided by a p-n junction diode that consists of two types of semiconductors.

In this chapter the discussion starts from the properties of semiconductors, on the basis of that we can determine the highest amount of the solar energy that can be captured by a certain semiconductor. Thereafter the p-n junction is explained, and from the p-n junction we proceed to Photovoltaic cells and further to Photovoltaic modules and arrays. Some attention is also paid to the impacts of temperature and irradiance on the performance of a PV module. The measurement of the performance of PV module is then discussed.

2.2.Band Structure and Band Gap Energy

According to quantum mechanics, electrons in atoms have well-defined discrete energy levels. By combining number of atoms these levels spread out into so called bands. Depending on the distance of the atoms and the bonds between them, there might be bands of forbidden energy called band gaps between the atoms, or the bands may overlap, forming a continuum of allowed energy states in the material. The characteristics of insulators, conductors and semiconductors depend on their band structure [6].

Among all the bands, valence band is the one which holds importance; this is the band which is highly filled band, and the conduction band. But, in the valence band all the energy states are occupied and hence its electrons are immobile, whereas in the conduction band there are plenty of unoccupied states for electrons to move in response to an applied electric field. However, to get into the conduction band, an electron has to jump over a gap – the forbidden band between the valence and conduction bands [5]. Hence the conductivity properties of a material are dependent on the size of this gap, called the band gap energy. In conductors the valence and conduction bands overlap; thus there are lots of mobile electrons to carry a current already at lower temperatures. In insulators, the band gap energy at room temperature can be 5 eV or more, and in semiconductors it is around 1 eV (at room temperature). For instance the band gap energy of silicon is 1.12 eV [5].

In semiconductors not only the electrons in the conduction band can move and carry currents, but also the vacancies they leave to the valence band, called as holes. When an

electron is excited to the conduction band, a vacant energy state, a hole, is left behind in the valence band. Another electron can move into this hole, and further a third electron may move to the vacant state of the previous electron and so on. This apparent motion of holes in the valence band contributes to the current, like the motion of electrons in the conduction band. When an electric field is applied, the holes in the valence band move to opposite direction with respect to the electrons in the conduction band, although the moving charge carriers are actually electrons in both bands. This feature, observed in pure semiconductors, is known as intrinsic conductivity [2], [5].

Now it is important to know how an electron can obtain the required energy to jump to the conduction band. Thermally is obviously one way, but in photovoltaic the energy is received from the photons of solar radiation. To excite an electron for instance in a silicon crystal, a photon with energy of 1.12 eV is required. The energy of a photon is related to its frequency with the following expression:

$$E = hv = h\frac{c}{\lambda} \tag{2.1}$$

where h is known as the Planck's constant (6.626 * 10^{-34} Js), v is known as photon's frequency (Hz), ג is its wavelength (m) and c is known as speed of light (2.998 * 10^{8} m/s). The speed of light is related to the frequency and wavelength with the expression c = vג [2].

Using equation 1.1 it can be calculated that in silicon, photons with wavelengths shorter than 1.11 μm are able to excite an electron to the conduction band. If the wavelength of Photons is longer than 1.11 μm they cannot do this, so their energy is wasted as heat [1]. Moreover, as only the exact amount of 1.12 eV is utilized by the excited electron, photons with wavelengths shorter than the limit have excess energy that also heats the cell. This means that in the case of silicon 20.2% of the sun's energy is wasted due to photons with too long wavelengths, and 30.2% due to photons with too short wavelengths, giving a theoretical upper limit of 49.6% for the efficiency of a single junction silicon solar cell, it is shown in the figure 2.1 [1]. In real silicon solar cells, however, the highest efficiencies that have been obtained in laboratories are in the order of 25%. The remaining 20% is lost due to various reasons, such as [1]:

- some of the photons pass right through the cell and few of them are reflected from the surface of the cell
- part of the generated electron-hole pairs are recombined before they contribute to the current
- the cell has some internal resistance.

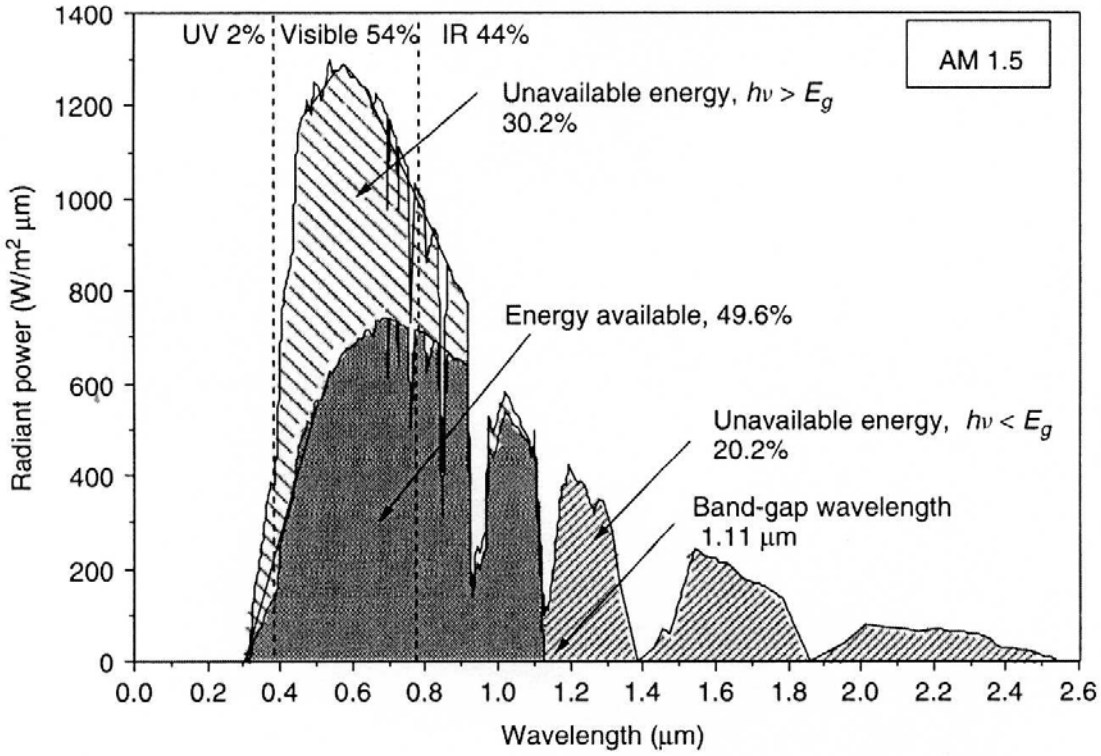

Figure 2-1: The solar spectrum at AM1.5

Thus, it is the size of the band gap of the material used that determines the theoretical upper limit for the solar cell's efficiency. If the energy of the band gap is low, there are more photons with the ability to excite electrons to the conduction band, resulting in a higher current; on the other hand, there are also more photons with excess energy that is wasted as heat. In turn with higher band gap energy, fewer electrons are excited, but the electrons have more energy and there is low number of photons with excess energy that is to be dissipated. Thus, a smaller band gap yields more current and low voltage, and a higher band gap gives the opposite. The optimum band gap, that results in the highest possible power and efficiency is estimated to be between 1.2 eV and 1.8 eV [2] – the

band gap of silicon is thus slightly too small. When new photovoltaic materials are developed, the size of the band gap is one of the primary concerns.

2.3.Doping

As stated earlier, semiconductors are doped to improve their conductivity and to get the required constituent for the p-n junction that is the p- and n-type semiconductors. N-type silicon is developed by introducing a small portion of group V element, typically phosphorus, into the silicon crystal. Typically a ratio is approximately, one phosphorus atom per 1000 silicon atoms, and this is sufficient to change the conductivity properties of silicon significantly. A phosphorus atom takes place of a silicon atom in the crystal lattice, and four out of the five valence electrons of phosphorus, form the covalent bonds to the adjacent silicon atoms [2] [5]. However, the fifth electron, is very loosely bound, and requires very little energy to be excited to the conduction band; at room temperature the fifth electron is most probably found in the conduction band. Thus, the fifth electron then leaves behind is a, +15e phosphorus nucleus surrounded by 14 electrons, i.e., an ion with a net charge of +e. This ion is fixed in the crystal lattice – hence there is a fixed net positive charge and a free electron towards each ion. As group V elements donate electrons, they are called donors. This type of semiconductor is called an n-type semiconductor because of the mobile negative charge carriers. [2], [5].

To fabricate p-type semiconductor, group III elements are introduced to the semiconductor. Silicon is typically doped with boron, with approximate concentrations of one boron atom per ten million silicon atoms [1] [5]. Again, each boron atom substitutes

a silicon atom in the silicon crystal, and is surrounded by four silicon atoms [1] [5]. Boron has three valence electrons that are all bound to the adjacent silicon atoms, but an extra hole is left vacant, a vacant energy state, is left next to the boron atom [1] [5]. This hole can be easily filled by electrons from nearby atoms, and can therefore be thought as a mobile positive charge. As the hole is filled, the boron atom having a +5e charge in its nucleus is surrounded with six electrons – thus a fixed ion with net charge $-e$ is formed. As boron atoms accept electrons, they are called acceptors. A semiconductor doped with an acceptor is called p-type semiconductor because of its free positive charge carriers. [1], [5]

It is important to remember that despite their names, p- and n-type semiconductors are electrically neutral. The names merely refer to the type of majority charge carriers in these materials – electrons in n-type and holes in p-type semiconductors.

2.4.The p-n junction

When p- and n-type semiconductors are brought into contact, in the vicinity of the junction, the electrons from the n-side diffuse to the p-side and combine with the holes. Due to these phenomena, electrons create immobile negative ions to the p-side and leave immobile positive ions behind in the n-side. This creates an electric field that is directed from n-side to p-side and thus opposes the diffusion of electrons. Finally equilibrium is attained, and no diffusion of electrons occurs. Consequently, the p-n junction diode is divided into two regions: a depletion region and the quasi-neutral regions. As illustrated in figure 2.2, depletion region encompasses the region in the immediate vicinity of the junction, which is – due to the diffusion described above – depleted from charge carriers.

Quasi-neutral regions in turn cover the regions “far” from the junction on both sides. In these regions the space charge density is assumed zero (hence the name quasi-neutral region) since no electrons have diffused from or to these regions to create positive or negative ions [7, 8].

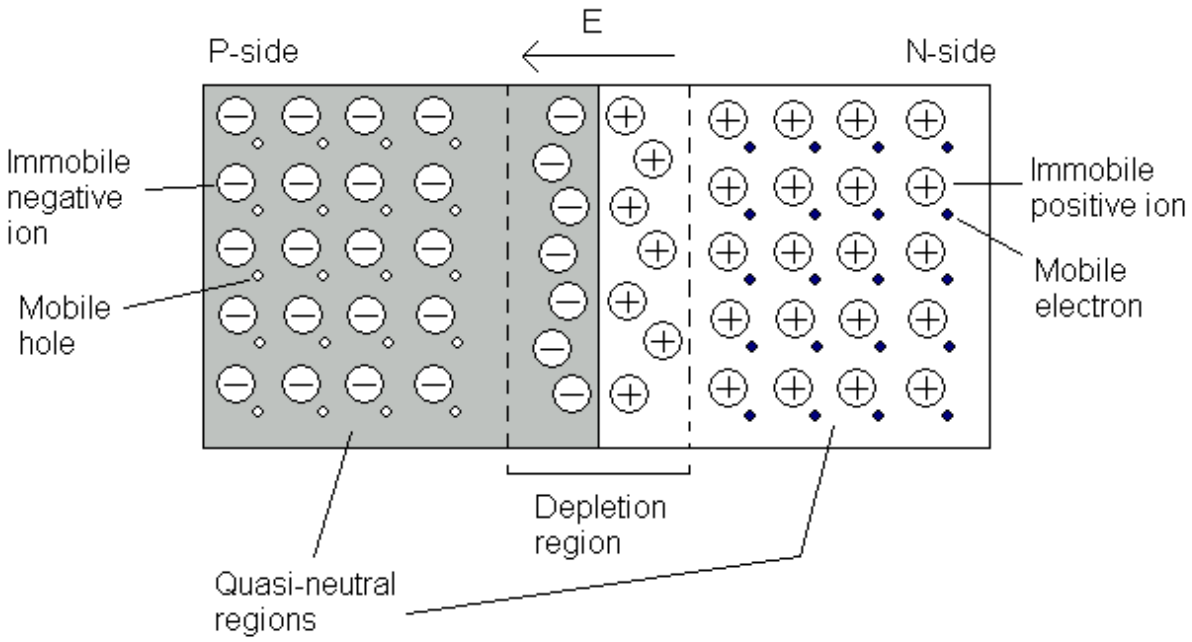

Figure 2-2: The p-n junction

The impact of the photovoltaic modules like, voltage rise due to reverse power flow from the PV system and harmonics at the point of common coupling (PCC) are studied for the real integrated system is discussed in “Advanced Analysis of Clustered Photovoltaic System’s Performance Based on the Battery-Integrated Voltage Control Algorithm” and “Performance Assessment of the Inverter-based Grid Connection of Photovoltaic

Systems" [1], [20]. A SIMULINK model is developed which consists of seven busses and photovoltaic model is integrated at the seventh bus.

2.5. Types of Photovoltaic Cells

There are two types of PV cells they are:

- Polycrystalline Silicon Cell
- Amorphous Silicon Cell

Polycrystalline Silicon: Polycrystalline silicon (polySi) physically differs from single-crystal silicon in such a way that it is a combination of many grains of single-crystal silicon. The size and quality of the grains determine their effect on solar cell performance: the larger and more perfect the grains are, their electrical behavior resembles that of a cell made from single-crystal silicon.

The problem with using grains is that when light-generated charge carriers strike the boundaries between the grains they lose their Kinetic Energy. Because there are fewer grain boundaries in material when the grain size is large, larger grains mean better cell performance. Another way to ensure that charge carriers encounter fewer grain boundaries is to orient the grains so that they stand vertically like columns, with no grain boundaries crossing the cell parallel to the junction. Since charge carriers in an operating cell tend to flow from top to bottom, a cell whose grains are wide vertical columns is similar to a group of smaller single-crystal cells packed together. In actual cells, horizontal boundaries are not eliminated but can be restricted to the extent that their effect is reduced.

Polycrystalline silicon solar cells have efficiencies over 10%, and they are suitable for long-run reliability, with decreased raw material and crystal sheet preparation costs.

Amorphous Silicon: In comparison to single-crystal or polycrystalline silicon, amorphous silicon's atomic structure is disordered. Until 1974, amorphous silicon was thought to be totally inappropriate for photovoltaic use because of its structural and electrical properties are similar to that of glass (an insulator) than those of crystalline silicon or similar semiconductor materials. However, by properly controlling the conditions under which it is deposited and by carefully modifying its composition, amorphous silicon can be used in solar cells. In fact, amorphous silicon, although still poorly understood in many respects, has become one of the leading candidates for future PV power generation from flat-plate systems for direct sunlight.

One of the main barriers to amorphous silicon's being a good photovoltaic material is the presence of dangling bonds. Dangling bonds, whether from the disorder of silicon atoms or from the presence of non-silicon impurity atoms, impede the free passage of charge carriers. For instance, a free electron could encounter a dangling bond, be attracted and held by it thereby losing kinetic energy of the movement. This is known as *trapping.* The electron can subsequently recombine with a hole. But if amorphous silicon is deposited in such a way that it contains hydrogen concentration of 5-10%, the hydrogen atoms form chemical bonds with some of the dangling bonds, removing them. Removing dangling bonds results in a small but extremely important enhancement to the freedom of movement of electrons and holes in amorphous silicon.

However, the mobility of electrons and holes in hydrogenated amorphous silicon are still very poor compared with mobility in crystalline silicon.

2.6.Advantages of Photovoltaic

The Photovoltaic systems got considerable advantages over conventional power sources:

• Reliability: Photovoltaic systems reliability is proved even in harsh conditions. PV arrays can be used as backup electrical power source in situations when there is load shedding.

• Durability: Even after ten years of use most PV modules available today show no degradation. It is likely that future modules will generate power for than twenty five .

• Low Maintenance Cost: Since PV systems require only intermittant inspection and occasional maintenance, these expenditures are usually less than with traditionally fueled systems. And moreover, transporting materials and personnel to remote areas for equipment maintenance or service work is inexpensive.

• No Fuel Cost: As the Photovoltaic generators work on solar energy so no fuel source is required, hence there are no costs associated with purchasing, storing, or transporting fuel.

• Reduced Sound Pollution: Photovoltaic systems don’t emit high volumes of sounds while operation.

• Safety: As Photovoltaic modules do not use the combustible fuels, hence they are very safe when properly designed and installed.

• Electrical Grid Decentralization: The Small-scale decentralized power stations mitigate the possibility of breakdowns on the electric grid.

• High Altitude Performance: The Increased solar irradance at high altitudes makes using photovoltaic’s advantageous, since power output is optimized. In contrast, a diesel generator at higher altitudes is de-rated since there are losses in efficiency and power output.

2.7.Disadvantages of Photovoltaic’s

Photovoltaic’s have some disadvantages when compared to conventional power systems:

• Initial Cost: The initial cost of the Photovoltaic system is high that makes it less popular.

• Variability of Available Solar Radiation: The Weather plays important role in deciding the power output of any solar-based energy system. If there are variations in climate or site conditions these require modifications in system design.

• Energy Storage: Most of the Photovoltaic systems use batteries for storing energy, thus increasing the size, cost, and complexity of a system.

• Education: As Photovoltaic systems present a novel technology. Only few people can understand their value and feasibility. Thus, this lack of information slows market and technological growth.

2.8.Building of Large PV Arrays

The single PV cell has limited output. Individual cells can be used to power small equipments such as toys, watches, and pocket calculators. But to provide reasonable power for many practical applications, voltage and amperage output from the PV source must be increased.

Some of the factors that must be managed are the variability of individual-cell energy output which can worsen with age and potential problems with the integrity of the connections linking one cell to another. Besides these problems, which are tied to the cell itself, the designer grouping PV Cells in a large terrestrial installation must account for uneven illumination such as caused by cloud shadows, for example.

2.9.Boosting Voltage and Amperage

Ideally, connecting individual cells in parallel that is; tying a common lead to all positive cell terminals and another lead to all negative terminals under proper conditions can produce an amperage output from the group of cells that is the sum of that from the individual cells. There is no voltage increase. In a very real sense, combining cells in parallel is equivalent to making a cell larger.

Also under ideal conditions, when solar cells are joined in series that is, when the positive lead from one cell is joined to the negative of the next, and so on the voltage contribution from each cell adds. The total current available from integrating the cells in this way is no more than from an individual cell.

The basic component of a PV system is the photovoltaic cell. Multiple cells are connected in series and parallel to form solar panels or modules, which are sold commercially for applications such as grid tied solar generation. Solar modules are connected in series and parallel in order to create a PV array. The solar array produces DC power which for grid tie systems must be adjusted by a maximum power point tracker (MPPT) and then converted to AC by a DC to AC inverter. These functions are performed by the power conditioning unit (PCU) which is composed of the MPPT and inverter.

2.10. Worldwide Installation of PV

The total photovoltaic (PV) installations of the world were 2.826 gigawatts peak (GWp) in 2007, and it rose to 5.95 gigawatts in 2008, a 110% increase. The countries that are

leading are (Germany, Japan and the US), they represent nearly 89% of the total worldwide PV installed capacity. According to Navigant Consulting and Electronic Trend Publications, the estimated Photovoltaic worldwide installations in the year 2012 will be 18.8GW. The table below shows the worldwide installation of Photovoltaic generators descending order.

S. No.	Capacity (GW)	Location	Year of Construction
1	60	Spain, Olmedilla, (Castilla-La Mancha)	2008
2	54	Germany, Straßkirchen	2009
3	53	Germay, Turnow-Preilack	2009
4	50	Spain, Puertollano, (Castila-La Mancha)	2008
5	46	Portugal, Moura, (Alentejo)	2008
6	45	Germany, Köthen	2010
7	42	Germany, Finsterwalde	2009
8	40	Germany, Brandis	2008
9	34.5	Spain, Trujillo, (Cáceres)	2008
10	34	Spain, Arnedo, (La Rioja)	2008
11	31.8	Spain, Dulcinea	2009
12	30	Spain, Merida, (Extremadura)	2008
13	26	Spain, Fuente Alamo, (Murcia)	2008
14	25	USA, Arcadia, FL	2009
15	24.5	Germany, Finow	2010
16	24	Germany, Montalto di Castro, (Lazio)	2009
17	24	Korea, Sinan	2008
18	23.4	Canada, Sarnia,(Ontario)	2009-2010
19	23.4	Canada, Amprior, (Ontario)	2009
20	23.2	Spain, Lucainena de las Torres, (Almeria)	2008

Table 2-1: The list of the major PV power stations in the world is given in the following table.

2.11. Problems associated with PV Arrays

If the electrical performance of each cell is the same, then it makes no difference how the strings and groups are ordered in achieving a desired output. Unfortunately, actual cells vary in quality: Even under like conditions of illumination, not all cells behave alike. Inherent cell-to-cell differences are aggravated by uneven illumination. Even worse, if some cells fail and lose their ability to function altogether, they may block current flow like an open electrical switch. Others break down and become, for all purposes, a minimum, such effects lead to reduced array output. At their extreme, such effects can cause the destruction of an array because of an overheating.

The effect of such breakdowns and some other performance irregularities in a solar array can be minimized by inserting appropriate electronic components into the module circuitry. One precaution against single-cell breakdown's affecting other areas of the module is to place solid-state diodes either in line with or across a string of cells at appropriate junctures. The use of diodes can cut into electric-energy output when all of the module's cells are properly functioning. In such cases they represent an unwanted load.

2.12. Problems due to the integration of Photovoltaic Generators with the power system

There is tremendous increase in the penetration of the Photovoltaic generators (PV Generators) in countries like Japan, Germany, Spain and other countries. According to different studies conducted by the European PV industry association (EPIA) [3], the grid

connected system was growing more rapidly than the standalone PV Generators. But the drawback for the large scale integration of the PV generators is its high investment cost and the existing structure of the energy markets.

Based on the data collected and from the practical experience of world PV cluster systems, the major system impacts due to integration of large PV generators at the point of common coupling (PCC) includes voltage variations, current and voltage harmonics, increase on short circuit capacity, grid islanding protection, and other power quality issues, such as flicker and stress on distribution transformer. For instance, the PV cluster demonstration site at Gunma, Japan has suffered from the voltage rise problem, and the PV system in Freiburg area of Germany experienced voltage variation problem [3].
Actually, there is no unique definition of a clustered PV system. In general, if the density of PV Generators installations in an area or community is high, the system can be called as the cluster PV system [3].

In the PV systems, voltage at the PCC on the power distribution line will rise because of the reverse power flow from each PV system on clear days, especially if the amount of integration of PV generation is large [3].

If this trend of increasing the integration of the PV Generators continuous for the long it would bring serious voltage rise problems in future [3].

Large integration of PV Generators would increase the short circuit capacity of the network thus the fault current which will in turn affect the coordination of the protective devices [4].

In “Improved Circuit Model of Photovoltaic Array” [3], a photovoltaic model is developed and it is used to analyze the PV curve (Power versus Voltage curves) for a mismatched PV panel that is when different cells or whole panel is exposed to different solar irradiance when connected in series.

In “Design and Simulation of Photovoltaic Super System with Simulink” [6], the design and simulation of the PV model is discussed, the model is developed using SIMULINK. The developed model includes solar photovoltaic array, maximum power point tracker (MPPT), battery, charger, DC/DC converter and Load. The model is simulated under four testing scenarios including sunny, cloudy conditions and constant, varying loads.

Several studies have been carried out to develop and analyze the impact of Photovoltaic distributed generator. An approach is defined in “Development of a photovoltaic array model for use in power electronics simulation studies [9]” in order to develop a complete solar photovoltaic power electronic conversion system for simulation. To this an approach chosen for the modeling was from the perspective of power electronics that is to design overall model in terms of the manner such that electrical behavior of the cell changes with respect to the environmental patterns like solar irradiance and the cell temperature. The model developed depends on the change in solar irradiance and the cell temperature.

A circuit-based photovoltaic module electrical standalone model is developed based on Shockley diode Equation [1] in Matlab for a typical 60W solar panel. The model developed estimate the electrical behavior of the cell with respect to the change in temperature and solar irradiance. The developed model calculates the output current for a given open-circuit voltage provided with solar irradiance and the temperature of the cell. All these are discussed in “Model of Photovoltaic Module in Matlab™ [10]”. The results obtained from this model were compared with the manufacturer’s published curves and show excellent correspondence to the model.

A generalized photovoltaic module is developed in “Development of Generalized Photovoltaic Model Using MATLAB/SIMULINK [11]” using SIMULINK which represent a PV cell, module or an array for easy use on the simulation platform. This makes the generalized PV model easily simulated and analyzed in conjunction with power electronics for maximum power point tracker. The developed model takes into consideration the affect of the sunlight irradiance and cell temperature.

In [12], a report is presented on modeling and simulation of a stand-alone photovoltaic system connected to a battery bank and it is compared with the system installed at the Riso National Laboratory. The model developed is made up of the blocks in order to facilitate modeling of other structures of PV systems.

A photovoltaic module electrical model is developed in “Evaluating MPPT convertor topologies using a MATLAB PV model [13]” using MATLAB and this model is used to investigate variation of maximum power point with temperature and insolation [13]. Then a comparison of buck versus boost maximum power point tracker (MPPT) topologies is made, and further it is compared with a direct connection to a constant voltage (battery) load. The effect of shunt resistance is excluded in the study [13].

A model for PV panel is constructed in “Modeling and a MPPT method for Solar Cells” using MATLAB and it is used to track the maximum power point (MPPT) using constant voltage control method. The model developed takes into account the series and shunt resistances of the panel. Moreover, it also takes into account the solar irradiance and cell’s temperature [14].

The advantages of the PV generator such as cost-effectiveness, environment friendly and less data storage space requirement are discussed in “Mathematical Modelling and Performance Evaluation of a Stand-Alone Polycrystalline PV Plant with MPPT Facility” [16]. Moreover, a model of polycrystalline PV array is developed using SIMULINK, and its performance under various loading conditions and whether conditions furthermore the model is used to develop a load shedding scheme for a stand-alone PV system [16].

In “Optimized Photovoltaic Solar Charger with Voltage Maximum Power Point Tracking” [18], photovoltaic module is used to charge the Lithium-ion (Li-Ion) batteries. It is implemented on a conventional Pulse Width Modulator (PWM) duty cycle ratio

control method to design a solar battery charger. MPPT is used so that the output power is maximize irrespective of cell temperature and solar irradiance.

Power quality problems associated with the large integration of PV generators connected to the PCC with an inverter are investigated in “Harmonic Interaction between a Large Number of Distributed Power Inverters and the Distribution Network” [21]. The main objective of this research is to study the observed phenomena of harmonic interference of large populations of these inverters and to compare the network interaction of different inverter topologies and control options [21]. And moreover, the power quality problems are investigated using laboratory experiments and computer modeling of different inverter topologies [21].

In “Technologies for the New Millennium: Photovoltaics as a Distributed Resource” [22], types of Photovoltaic systems, benefits of PV systems and interconnection issues related to the PV system are discussed. Further IEEE Std. 929 that is: “Recommend Practice for Utility Interface of Photovoltaic Systems.” And the solutions for the interconnection issues are discussed.

A case study is conducted for a 100 KWp PV generator in “Impact of large Photovoltaic penetration on the quality of the supply: A case study at a photovoltaic noise barrier in Austria” [23], situated in Gleisdorf Austria. The parameters that were measured are voltage variations, voltage dips and swells, flicker, harmonics unbalance etc. were measured and analyzed according to the standard EN50160. That is “Voltage

Characteristics of electricity supplied by public distribution systems". A detailed study of the network configuration was performed in order to perform comprehensive analysis of the measurements. As a result typical values of the total harmonic distortion or flicker level are set.

The problems associated with the penetration of PV generators in the urban power system are discussed in "Electrical Impact of Photovoltaic Plant in Distributed Network" [24]. A single line network is simulated in order to evaluate the relation between number of PV systems installed along the line and maximum PV power that can be installed. Then the problems associated with the PV penetrations are examined concerning a clustered PV system installed in the city of Torino, Italy.

In "A Novel Integrated Renewable Energy System Modelling Approach, Allowing Fast FPGA Controller Prototyping" [25], both photovoltaic and wind generators were first simulated in Matlab then it was holistically modeled and implemented in FPGA (Field Programmable Gate Array**)** using Celoxica's Handel-C software. Then the developed models were compared for the mismatch. The holistic model developed was used for prototyping the global digital controller. And it is used for real time verification of the data. When photovoltaic modules are connected to the grids.

Experimental analysis is performed to evaluate the affect of clustered photovoltaic modules on the power quality of the grid. Several parameters as voltage and current distortion, flicker, voltage variations at fundamental frequency and power factor have been observed and compared with the standards, all this is discussed in "Comparison of

Power Quality Impact of Different Photovoltaic Inverters: the viewpoint of the grid", [26].

In [27] and [28] the affect of Distributed Generators (DG) on protective device co-ordinations such as fuse-fuse, fuse-recloser and relay-relay are discussed. And in each case, depending on size and placement of DG, some margins are set, in which the coordination may hold and certain cases, where no margin is available are also listed.

In "Analysis Results of Output Power Loss Due to the Grid Voltage Rise in Grid-Connected Photovoltaic Power Generation Systems" [29], a voltage regulator, Power Conditioning unit (PCS) is described, and occurrence of output power loss due to grid's overvoltage is summarized. PCS will regulate its output power flow if the voltage becomes higher than the upper limit in order to avoid the overvoltage at the power grid. Thus, in other words PCS will not generate electricity under the high grid voltage. The regulation of output power from PCS is done by measuring the values current, voltage and power both input DC and output AC terminals. Based upon the measured values the PCS will decide whether to allow or to stop the output power. In this analysis a demonstration projected was selected, it consists of 553 residential PV systems; the installed capacity of this PV system is 2.1 MW. It was found that only a small number of PV systems experienced a considerable amount of output power loss due to high grid voltage on a particular day; however other system's outputs also contribute for the voltage rise. The causes for this uneven distribution of output energy loss are due to, difference in line impedance, difference in the setting of the starting voltage of the PCS's

grid overvoltage protection function and unbalanced load of the single phase three wire systems.

The reduction in output power from the PV system due to overvoltage of the power distribution line is studied in “Detailed performance analyses results of grid-connected clustered PV systems in Japan – first 200 systems results of demonstrative research on clustered PV systems” [30]. In this paper the factors that are responsible for the overvoltage like PV system’s output power and light load especially during weekend are discussed. Simulation results showed that both the output from the PV system and light load raise the voltage of the line approximately by 2V, which in turn substantially reduce the output power of the PV system.

CHAPTER 3

3.System Modeling

3.1.System Description

The system modeled in this work consists of five major sub-systems they are: PV generator model, Charger Unit, Battery, Inverter and the distribution system. In this chapter these sub-systems are briefly introduced, detailed modeling of these sub-systems is considered in the next chapter.

PV generator model: The PV generator directly converts the sunlight falling on it to the electricity. The PV generator considered in this work, at first consists of 72 mono-crystalline cells from Suntech connected in series. This PV generator produces an output power of 170W at 44.4V. (More technical specifications can be consulted from annex 1).

The charger unit: This sub-system is made up of two sub-systems they are: Maximum Power Point Tracker (MPPT) and DC/DC Charger. The power generated by the PV module is first fed to the MPPT the function of MPPT is to maximize the output power of PV module irrespective of the Sun's irradiance and Cell's temperature. The DC/DC converter is controlled by a PWM signal. The DC/DC converter is formed by two switches and an input and output filter.

Battery: The battery used in this work is rechargeable LI-ion battery. The purpose of the battery is to store the power generated from the PV generator. The stored power can be used by local DC load or the AC load by converting it into AC with the help of inverter.

Inverter: The inverter used in this work is the 2-arm IGBT diode bridge; it is used to convert the DC power of the battery to AC. The inverter gate signals are fed from a Discrete PWM signal generator. The carrier frequency of this PWM is set as 1080Hz.

Distribution System: In this work, a real distribution network is considered for analysis. The distribution network consists of an Utility system which generates power of 25MVA at 69KV. This voltage is step-down to 11.4KV with the help of an three phase transformer T1 (25MVA, 69KV/11.4KV), the PV generator feeds power to the bus 7 which is in-turn connected to distribution sub-station in the residential area through a pole mounted transformer T2 (1ϕ, 167KVA, 6.58KV/220V), the function of the transformer T2 is to transform the voltage of the distribution line from 6.58KV to 220V.

3.2.The Photovoltaic Cell

The photovoltaic cell is a semiconductor device which behaves as a current source when driven by a flux of solar radiation from the sun. This occurs when radiation is incident upon absorbing material and separates positive and negative charge carriers in the presence of an electric field. The electric field exists permanently at junctions or in homogeneities in solar cells which can be described as silicon semiconductor junction devices. A silicon semiconductor junction device contains a p-n junction similar to that of a common diode; however in a solar cell it exists over a large surface area. When not illuminated and connected to a forward bias the ideal solar cell mimics the electrical characteristics of an ideal diode as shown in Figure 3.1, modeled by the Shockley equation, where the current produced is referred to as the dark current I_D.

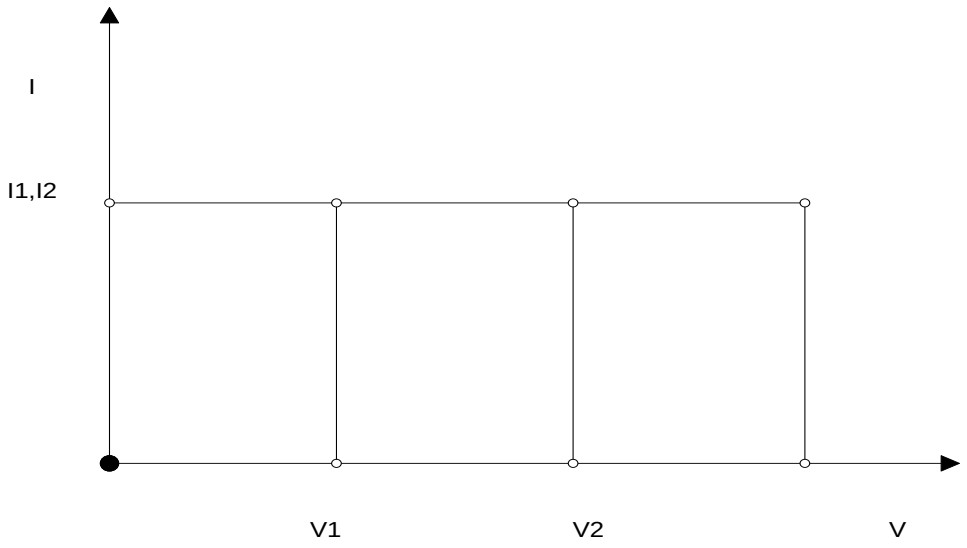

Figure 3-1: Ideal I-V curve for PV cell.

But in reality the I-V characteristics of a PV cell is different from the one shown in figure 3 but it will exhibit the characteristic shown in figure 3.2.

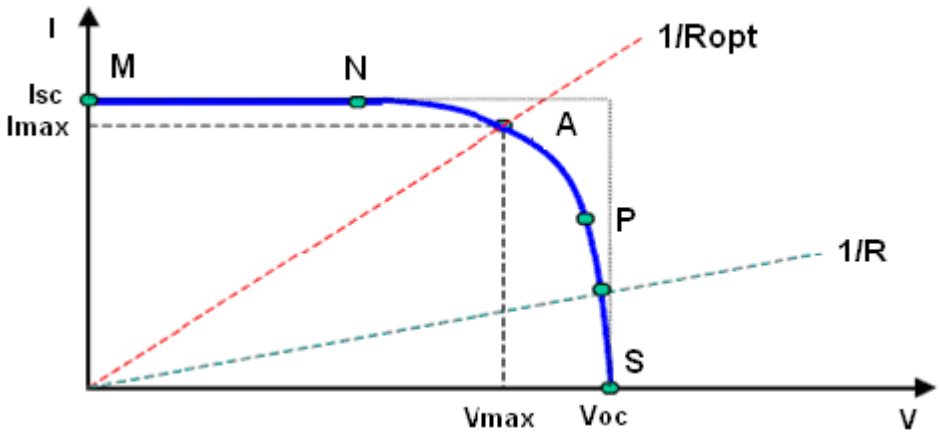

Figure 3-2: Typical I-V characteristic curve of a PV cell

The slight drop in the value of current between points M and A is due to, some of the current passing through the internal resistance of the PV cell. And between points A and S the load resistance increases forcing some of the current to flow through the diode resulting in the rapid drop in current to the load. This continues until point S where all the current flows through the diode and the internal resistance.

The operation of PV on this I-V curve is greatly determined by the insolation (irradiance), array open-circuit voltage, cell temperature and the load connected to the array. According to [23] by altering the amount of sun light that is available to the PV module the current that the module can produce is also altered. The current and power output of the solar panel is approximately proportional to illumination intensity (irradiance). Moreover, at a given intensity, the module voltage is determined by the characteristics of the load.

The effect of temperature on the output current of a PV cell is very small. By increasing the temperature a slightly higher current is produced, however this increase in temperature has a negative impact on the cell voltage. Increase in the temperature forces the diode in Figure 3.3 to conduct at a lower voltage therefore reducing the PV voltage where the curve collapses and greatly reducing the output power.

The effect of varying the load on the PV operating point can be explained using ohms law:

$$I = \frac{V}{R} \tag{3.1}$$

Figure 3.2 shows the load lines for different load resistance values. The slopes of these load lines are given by '1/*R*'. So, lower values of resistance results in steeper load lines and higher values of resistances result in flatter load lines. The operating point of the PV, connected to these loads is restricted to the intersection of the load line and I-V curve. Therefore, for a given sun's insolation (irradiance) there is only one load resistance that will produce maximum power and if the irradiance changes then the load resistance required for operation at MPP (maximum power point) also changes. But, the irradiance is not constant and it will change throughout the day therefore maximum power point trackers (MPPT) are needed to match the operating point to the load resistance.

A solar cell is usually represented by an electrical equivalent one-diode model with a series resistance, as shown in Figure 3.3.

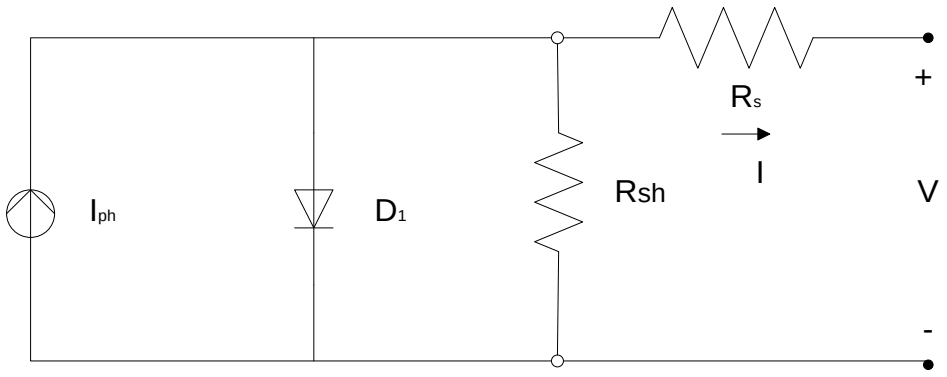

Figure 3-3: Electrical equivalent model of Solar Cell

The model contains a current source I_{ph}, one diode and a resistor R_s. The net current is the difference between the photocurrent I_{ph} and the normal diode current i_D. The diode current is given by (3.2).

$$i_D = I_0 * \left(e^{\frac{(V+R_s I)}{A v_T} - 1} \right) \tag{3.2}$$

Where:

$I_0 =$ diode current (strongly dependent on temperature);

$V =$ voltage imposed across the cell;

A= ideal factor (ideal: A=1; real: A>1);

$V_T =$ thermal potential given by (4.3);

R_s = Series cell resistance.

$$V_T = \frac{KT}{q} \tag{3.3}$$

Where,

'K' is the Boltzmann Constant, K= 1.38*10^{-23} J/K;

'T' is the cell temperature in Kelvin;

'q' is the electric charge of an electron, q= 1.6*10^{-19} C.

Thus, the characteristic voltage-current equation of a solar cell is given as:

$$I = I_{ph} - I_s[exp(q(V + IR_s)/KTA) - 1] - \frac{(V + IR_s)}{R_{SH}} \tag{3.4}$$

Where;

I_{ph} = light generated current or photo-current;

R_{SH} = shunt resistance;

I_s = the cell saturation current in dark

The photo-current mainly depends on the solar insolation (irradiance) and cell's working temperature, which is described as

$$I_{ph} = \left[I_{SC} + K_I\left(T_C - T_{ref.}\right)\right]^{\lambda} \tag{3.5}$$

Where;

I_{SC} = cell's short circuit current at 25° C and 1 KW/m^2;

K_I = cell's short-circuit current temperature coefficient;

$T_{Ref.}$ = cell's reference temperature

ג = solar insolation (irradiance) in KW/m^2;

On the other hand, the cell's saturation current varies with the cell temperature, which is described as:

$$I_S = I_{RS}\left(T_C/T_{ref.}\right)^3 exp\left[qE_G\left(1/T_{ref.} - 1/T_C\right)/KA\right] \quad (3.6)$$

Where;

$'I_{RS}'$ is the cell's reverse saturation current at the reference temperature and a solar radiation, and

$'E_G'$ is the band-gap energy of the semi-conductor used in the cell

It is to be noted that the shunt resistance R_{SH} is inversely proportional to the shunt leakage current to the ground [11]. Thus, the PV efficiency is insensitive to the variation in R_{SH} and the shunt-leakage resistance can be assumed to approach infinity without leakage current to ground [11]. On the other hand, if there is small variation in R_S it will considerably affect the PV output power. The appropriate model of PV solar cell with suitable complexity is shown in Figure 3.4 [11]. Equation (3.4) can be rewritten to be

$$I = I_{Ph} - I_S[exp(q(V + IR_S)/KTA) - 1] \quad (3.7)$$

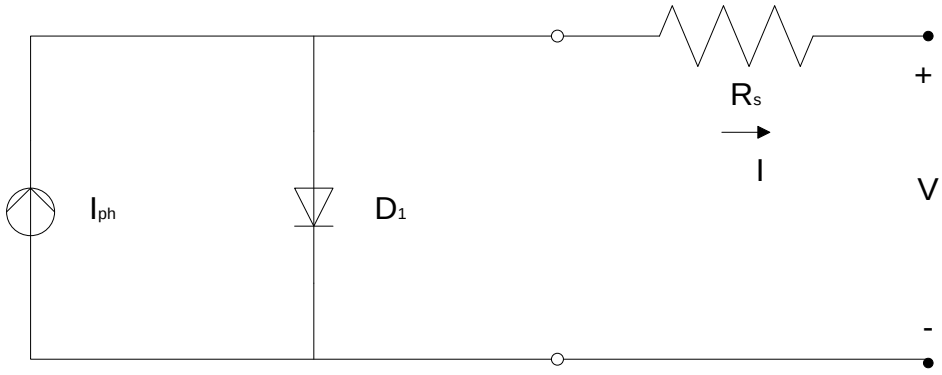

Figure 3-4: Appropriate Model

If we are considering an ideal Photovoltaic cell there is no series loss and no leakage to ground, that is R_S=0 and R_{SH}=∞. Thus, the above equivalent circuit of Photovoltaic cell can be simplified as shown in Figure 3.4. And, the equation (3.7) can be rewritten as

$$I = I_{ph} - I_S[exp(qV/KTA) - 1] \quad (3.8)$$

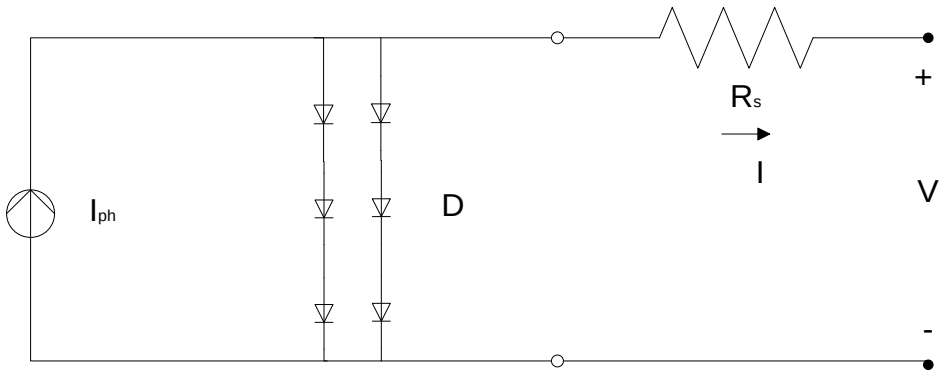

Figure 3-5: General Model of PV Module

3.3. The Photovoltaic Module

A photovoltaic module will be composed of a series and parallel combination of solar cells, with the additional components of blocking and bypass diodes. While the manufacture and size of solar cells vary, generally the voltage handling capability of a single cell will be relatively low on the order of 0.6 V [10]. In order to package solar cells as a more practical device most manufacturers produce solar modules; a group of solar cells connected in series and parallel in order to increase the voltage and current handling capability [10]. While a variety of connection schemes exist for a multitude of applications, a common scheme for PV modules used in grid tied power generation is a connection of 72 cells in series. As an example, the Suntech Power STP170S-24/Ac module which is so composed provides rated voltage and current of 44.4 V, 5.15 A.

In most PV design and modeling applications the following assumption is made, which is also used in this work:

1: Connection of solar cells in series will directly multiply the voltage handling capability of the system and connections in parallel will directly multiply current production.

For this assumption to be reasonable it is necessary for all solar cells to behave in a uniform manner, however it is clear that this is not always the case. Solar modules contain blocking and isolation or bypass diodes as shown in Figure 3.8 to reduce the effects of cells which do not act uniformly. Without these devices it is possible for cells or strings which are not operating uniformly to consume power generated by other cells or strings. These devices therefore reduce the power loss associated with non-uniformity and allow the behavior of the array to more closely resemble the uniform case by reducing the negative impact of non uniform cells.

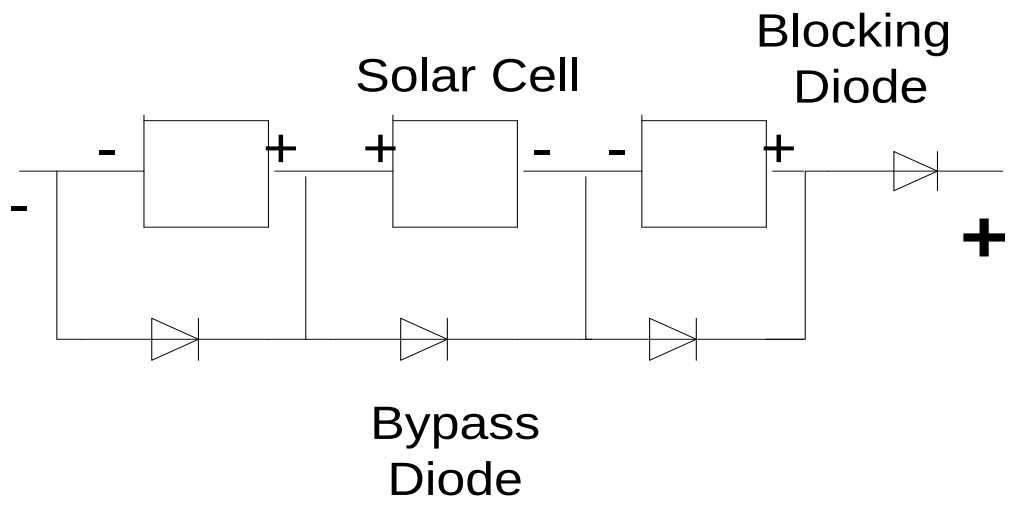

Figure 3-6: String of cells with bypass and blocking diodes

Thus for this work, the following additional assumptions are made:

2: Each cell behaves in a uniform manner. Under a given environmental condition the electrical characteristics of every cell in a solar array is identical.

3: For the purposes of modeling a solar array in this work the bypass diodes and isolation/blocking diodes are considered as ideal diodes.

With these assumptions in place, bypass diodes are reverse biased and act as open circuits while isolation or blocking diodes are forward biased and act as short circuits. Therefore it is not necessary to include these diodes in the mathematical model.

3.3.1. Bypass diode:

Bypass diodes are placed across each cell in a solar module in order to ensure that each series string of cells produces the maximum possible voltage. This protects against the case where a given solar cell does not receive the same illumination as other cells in the string. For example, given a string of cells, if a single cell is covered in dirt and thus absorbs less radiation it is possible for the voltage gain of this cell to reverse its direction which would significantly reduce the voltage gain of the entire string. Therefore, a bypass diode is connected in parallel to each solar cell which becomes forward biased if the voltage gain of a cell is reversed, and effectively creates a short across this cell. Then, when a cell voltage is reversed the voltage capability of the string is increased by the action of the bypass diode.

3.3.2. Isolation/Blocking Diodes:

Isolation or blocking diodes are often placed between each string of modules and the PCU in order to prevent module strings from absorbing power from the system when not illuminated. Under zero illumination and in the presence of forward voltage (provided by a battery, the grid, or other module strings) a string of solar modules will draw current from the circuit. Therefore isolation or blocking diode is placed between the module string and the voltage source as shown in Figure 3.6. The term blocking diode often refers to a single diode used in PV systems with battery storage, while isolation diodes refer to multiple diodes placed on the positive terminal of each series string of solar

modules. These diodes perform the same function of blocking a reverse current flow however multiple isolation diodes provide additional protection in the case of shading on a single string of modules. These diodes become reversed biased when the string is not illuminated thus preventing current flow to the string. In some cases, the function of a blocking diode is performed by switching in the PCU, however this only prevents the array from absorbing power from the grid, it does not prevent a single module string from absorbing power from the rest of the array.

3.4. The Photovoltaic Array

A Photovoltaic cell typically generates less than 2W of power at 0.5V approximately, so the cells are connected in series-parallel configuration on a module to produce enough power [11]. A Photovoltaic array is a group of numerous Photovoltaic modules which are electrically connected in series and parallel circuits to produce the required current and voltage [11].

A photovoltaic array is composed of series and parallel connections of solar modules. The number of modules connected in series and parallel is based on the voltage requirements of the system and the desired power output of the array. Grid connected systems require an inverter which in order to successfully interface with the grid requires a specific DC input voltage range generally on the order of 200-600 Volts DC. PV arrays are designed to produce a voltage close to the top of this range at rated power production. This allows the inverter to operate for the largest possible range of DC voltage input and therefore the largest range of environmental conditions.

Once the voltage requirement is met, power handling capability can be increased by connecting additional module strings in parallel [11]. This is done by first connecting the correct number of modules in series to fulfill the voltage requirement creating a string of modules. Next, additional strings of the same number of modules may be added to increase the current production and thus the power capability of the array [11]. It is important that each string is composed of an identical number of modules of the same brand and power rating. If strings are not matched the voltage production of each string may not be identical. In this case the voltage output of the array will be lower than that of the highest producing string; therefore the highest producing string does not operate at maximum efficiency [11]. Solar module's equivalent circuit arranged in N_P parallel and N_S series is shown in Figure 3.7. The terminal equation for the current and voltage of the array becomes as follows:

$$I = N_P I_{PH} - N_P I_S [exp(qV/N_S + IR_S/N_P)/KTA - 1] - \left(\frac{N_P V}{N_S} + IR_S\right)/R_{SH} \quad (3.9)$$

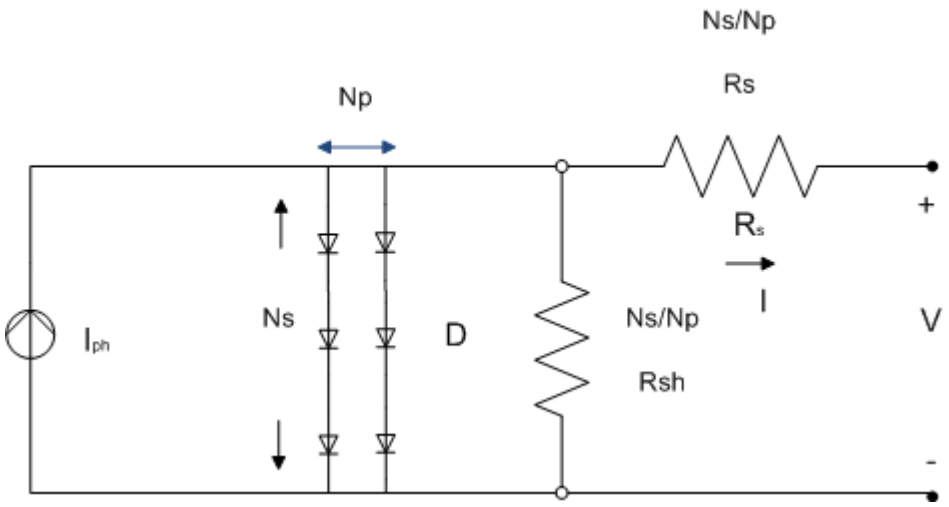

Figure 3-7: General Model of PV Module

As stated earlier, performance of the PV module mainly depend on the value of R_S, a small change in the value of R_S can fluctuate the efficiency of the PV module [11]. On the other hand, it is insensitive to the changes in the value of R_{SH}.Thus, for a Photovoltaic module or an array; the series resistance is of much importance and the shunt resistance moves towards infinity which is presumed to be open [11]. In commonly available Photovoltaic generators, generally PV cells are connected in series configuration so that the required working voltage is obtained. Then, they are arranged in series-parallel structure to achieve desired power output [11]. A suitable equivalent circuit for all PV cell, module, and array is generalized and expressed in Figure 10 [11]. For a PV cell N_S = N_P = 1, N_P =1 and N_S : series number of cells for a PV module, and N_S and N_P : series-parallel number for a PV array [11]. The mathematical equation of generalized model can be deduce as [11]:

$$I = N_P I_{PH} - N_P I_S[exp(qV/N_S + IR_S/N_P)/KTA - 1] \quad (3.10)$$

Thus, the most simplified model of generalized PV module is shown in Figure 3.8 [11]. And, the equivalent circuit is described on the following equation

$$I = N_P I_{PH} - N_P I_S[exp(qV/N_S\, KTA) - 1] \quad (3.11)$$

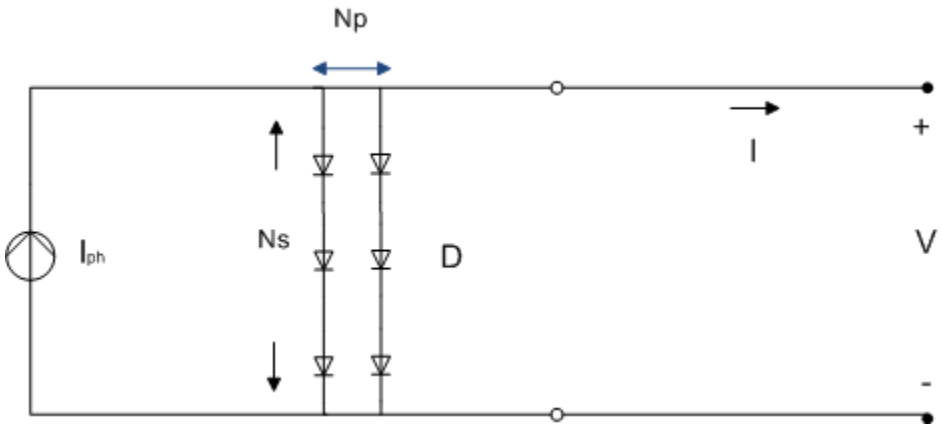

Figure 3-8: Appropriate Model of PV Module

3.4.1. Determination of PV Module Parameters

Manufacturer's specification of the Photovoltaic generators is the basis for determining most of the model parameters [11]. Among all the parameters the most important parameters widely used for describing the cell's electrical performance is the open-circuit voltage V_{OC} and the short-circuit current I_{Sc} [11].

The equations mentioned earlier are implicit and nonlinear; therefore, it is difficult to arrive at an analytical solution for a set of model parameters at a specific temperature and

irradiance [11]. Since normally I_{PH}>> I_S and by ignoring the small diode and ground-leakage currents under zero-terminal voltage, the short-circuit current I_{Sc} will beapproximately equal to the photocurrent I_{PH} [11], i.e.

$$I_{PH} = I_{SC} \tag{3.12}$$

And, the V_{OC} parameter is deduced by assuming the output current is zero. Given the Photovoltaic open-circuit voltage V_{OC} at reference temperature and ignoring the shunt-leakage current, the reverse saturation current at reference temperature is be approximately obtained as [11]

$$I_{RS} = I_{SC}/[exp(qV_{OC}/N_SKAT) - 1] \tag{3.13}$$

3.5.The Power Conditioning Unit

The power conditioning unit (PCU) is a device which interfaces the solar array with the utility grid. In a grid tie system without storage the PCU consists of a maximum power point tracker (MPPT) and a DC to AC inverter, as shown in Figure 3.9. In most cases the PCU also contains protection devices which disconnect the PV system from the grid in the case of grid failure. Many PCU's use the existing controllable switches of the DC to AC inverter in order to perform these protective functions. These components are described in detail in the following sections.

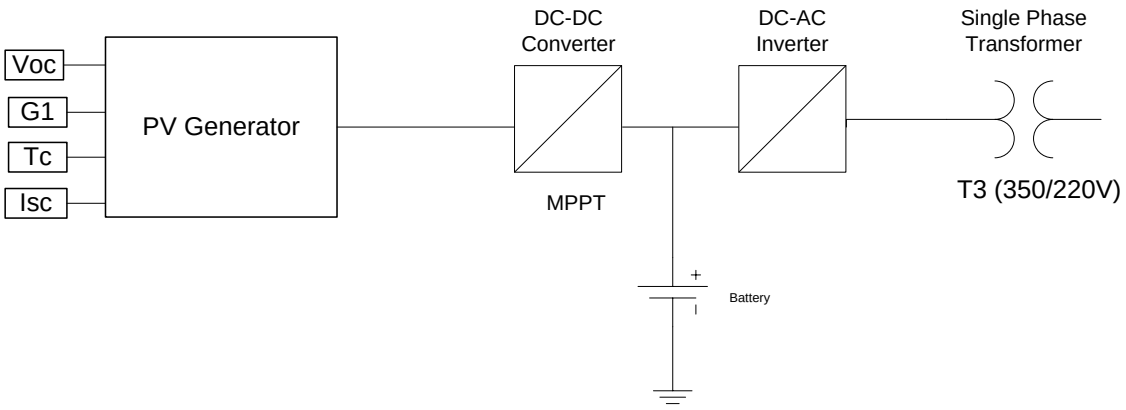

Figure 3-9: Components of the power conditioning unit

3.5.1. DC/DC Converter

A DC/DC converter consists of a number of storage elements and switches that are connected in a topology such that the periodic switching controls the dynamic transfer of power from the input to the output [16]. The storage elements are connected in such a way that they form a low pass filter to yield low output ripple voltage (less than 3%). In the designed system, there is also an input storage element that will allow the input ripple voltage to be less than 3% [16].

The two fundamental topologies of DC/DC converters that are widely used are the buck and the boost converter. There are many other topologies; most of them are derived from either the buck or the boost converter topology [16]. The main purpose of the DC/DC converter is to transform a DC voltage from one level to another. This is done by varying the duty cycle, δ. The duty cycle is defined as the ratio of the "on" duration to the

switching time period ‘T’ [16]. By varying δ the width of the pulses is varied and the concept of pulse width modulation, PWM is realized.

DC/DC converters have two distinct operating modes they are: Continuous Conduction Mode (CCM) and Discontinuous Conduction Mode (DCM). The converter can operate in either of these modes and each mode has extensively different characteristics [16]. The DC/DC converter is used for transmitting power from the solar Photovoltaic generator to the load and acts as an interface between the load and the module. The mode of operation of DC/DC converter considered in this thesis is Continuous Conduction Mode (CCM) [16].

3.5.1.1. Buck Converter Topology

There are five basic components of an ideal buck converter, namely a power semiconductor switch, a diode, an inductor, a capacitor and a PWM controller [16]. The topology of the buck converter is shown in Figure 3.10.

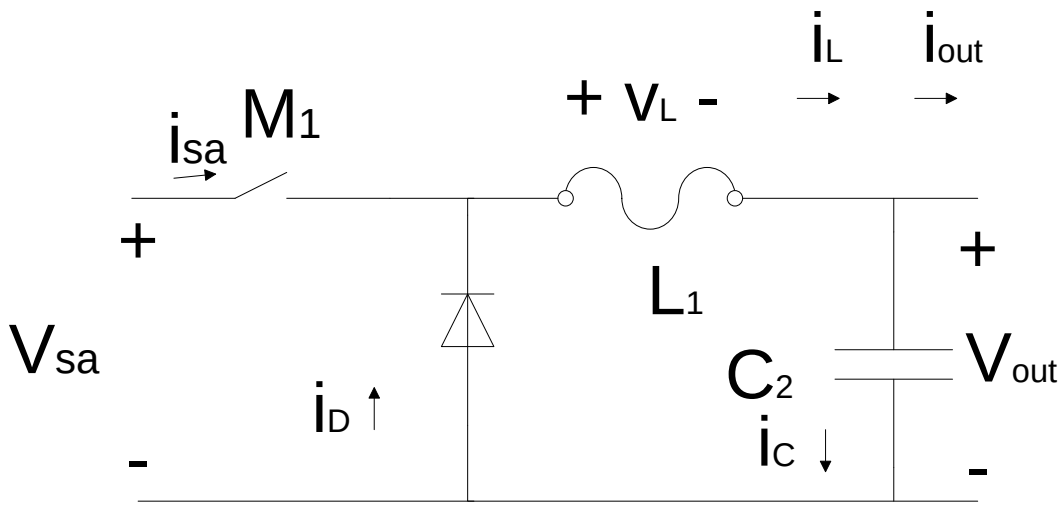

Figure 3-10: Electrical Model - DC/DC converter (Buck topology)

3.5.1.2. Theory of Operation

The DC/DC converter will connect / disconnect conveniently the solar panel from the battery based on PWM signals [16]. Taking into the account the idealized buck converter shown in Figure 3.11 and in order to simplify the results shown below, it is assumed that input voltage V_{sa} is ripple free [16].

The capacitor C is large enough such that v_{out} has a ripple of less than 3%, therefore it is basically ripple free. Current i_{out} is also assumed to be ripple free [16]. Assuming continuous conduction (e.g. i_L is always great than zero), the circuit has two topologies – switch M_1 closed and switch M_1 open. These steady states are shown in Figure 3.12 [16].

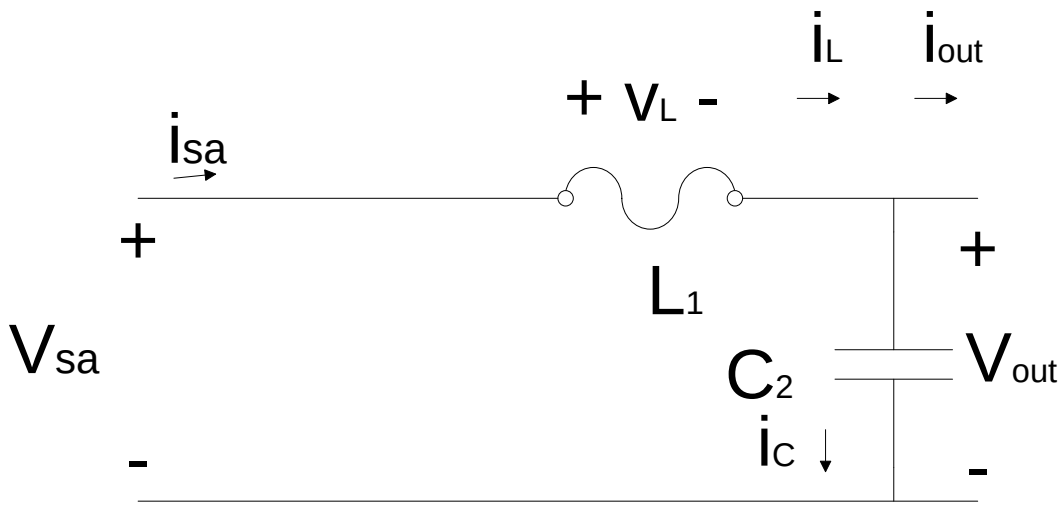

a) Switch M1 Closed

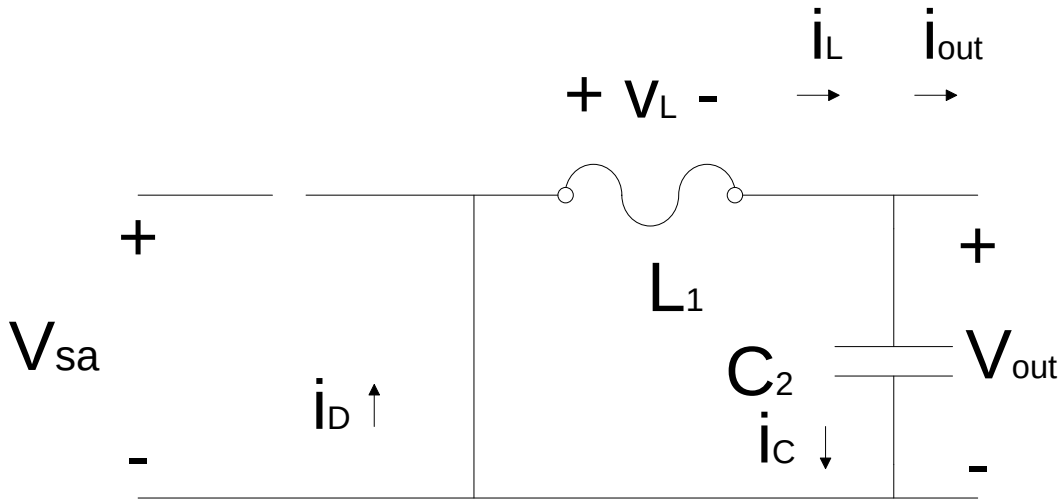

b) Switch M1 open

Figure 3-11: Switch Operation – DC/DC Converter

When the switch M_1 is closed, the power of the voltage source v_{sa} is delivered to the load through inductor L_1. Since the diode is in reverse bias mode so it will open, and the current i_L increases at the rate of:

$$\frac{di_L}{dt} = \frac{v_L}{L_1} = \frac{v_{sa} - v_{out}}{L_1}, 0 \leq t \leq \delta T \tag{3.14}$$

In this case the inductor L_1 is charging. When the switch is open, current i_L continues to circulate through the diode, and thus the diode is forward biased, and i_L decreases at the rate of:

$$\frac{di_L}{dt} = \frac{v_L}{L_1} = \frac{-v_{out}}{L_1}, \delta T \leq t \leq T \tag{3.15}$$

And the inductor L_1 is discharging. If the parameters of the circuit are well defined such that the current i_L does not go to complete zero (in this case the circuit is in continuous conduction), the diode remains in conduction until the switch closes and the diode is reverse biased and opens.

Due to the steady-state inductor principle, the average voltage v_L across L_1 is zero. Since v_L have two states, both having constant voltage, the average value is given by (3.16).

$$v_{out} = \frac{1}{T}\int_0^T v_{out}(t)dt = \frac{1}{T}\int_0^{\delta T} v_{sa}(t) = v_{sa}\delta \tag{3.16}$$

Therefore,

$$v_{out} = v_{sa}\delta \tag{3.17}$$

This relationship is very important because, it describes the operation of the buck converter. Over here 'δ' , is the duty cycle and varies between 1 and 0. Therefore the output voltage will always be less than the input voltage.

3.5.1.3. Sizing the output filter

Expressions (14) and (15) give the rate of rise and fall for current i_L . The average value of i_L is found by examining the node at the top of capacitor in Figure 12. Applying Kirchhoff's Current Law (KCL) in the average sense, and recognizing that the average current through a capacitor operating state is zero, it is obvious that:

$$i_{Lav} = i_{out} \tag{3.18}$$

From expressions (3.14), (3.15) and (3.18) one can draw a graph of current i_L , as shown in Figure 3.12.

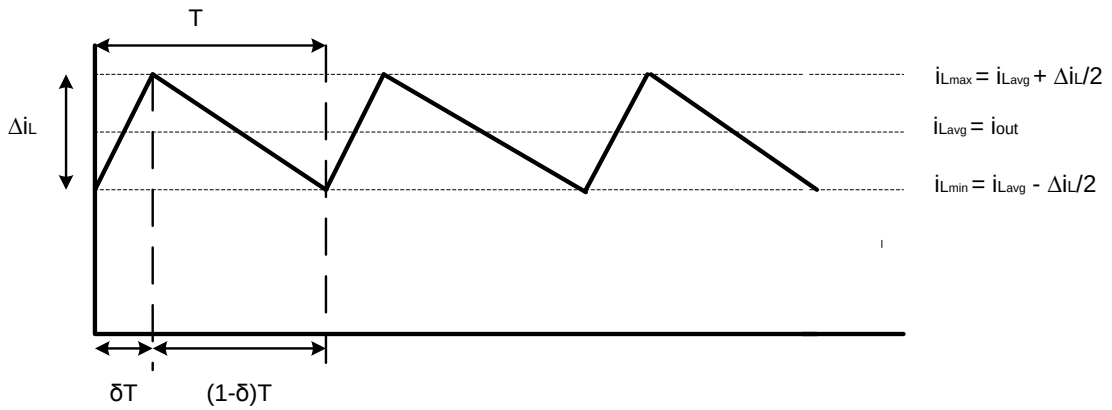

Figure 3-12: Inductor Current Waveform – Output Filter

Value of inductor L

Since the inductor current consists on straight line segments, it is possible to write the following expression:

$$i_{L_{avg}} = \frac{i_{L_{max}} + i_{L_{min}}}{2}, i_{L_{max}} = i_{L_{avg}} + \frac{\Delta i_L}{2}, i_{L_{min}} = i_{L_{avg}} - \frac{\Delta i_L}{2} \tag{3.19}$$

From (3.14),

$$\frac{di_L}{dt} = \frac{v_{sa} - v_{out}}{L_1} = \frac{\Delta i_L}{\delta T} \tag{3.20}$$

Thus,

$$\Delta i_L = \frac{v_{sa} - v_{out}}{L_1} \times \delta T = \frac{v_{sa} - \delta v_{sa}}{L_1} \times \delta T = \frac{v_{sa}\delta(1-\delta)}{L_1 f_{PWM}} \tag{3.21}$$

Where f_{PWM} is the commutation frequency. In the limit of the CCM, $\Delta i_L = 2i_{avg} = 2i_{out}$, such:

$$\frac{v_{out}}{L_{max}}(1-\delta)T = 2i_{out} \Leftrightarrow L_{max} = \frac{v_{out}(1-\delta)}{2i_{out}f_{PWM}} \tag{3.22}$$

The maximum value occurs when $\delta \to 0$. therefore,

$$L_{max} > \frac{v_{out}}{2i_{out}f_{PWM}} \tag{3.23}$$

This means continuous conduction for any value of duty cycle. v_{out} *a*nd i_{out} are the converter output voltage and current at the maximum input power and f_{PWM} is the switching frequency.

Value of the capacitor, C

The capacitor current, i_c is given by the difference between the current in the inductor and the load current i_{out} as follows:

$$i_c = i_L - i_{out} \tag{3.24}$$

From Figure 15, it can be deduced that each charging and discharging process is given by an equal area where it spends half of the period value $\left(\frac{T}{2}\right)$, and where each area represents a charge increment ΔQ of the capacitor.

$$\Delta V = \frac{\Delta Q}{C} \tag{3.25}$$

Where ΔV is the output ripple voltage.

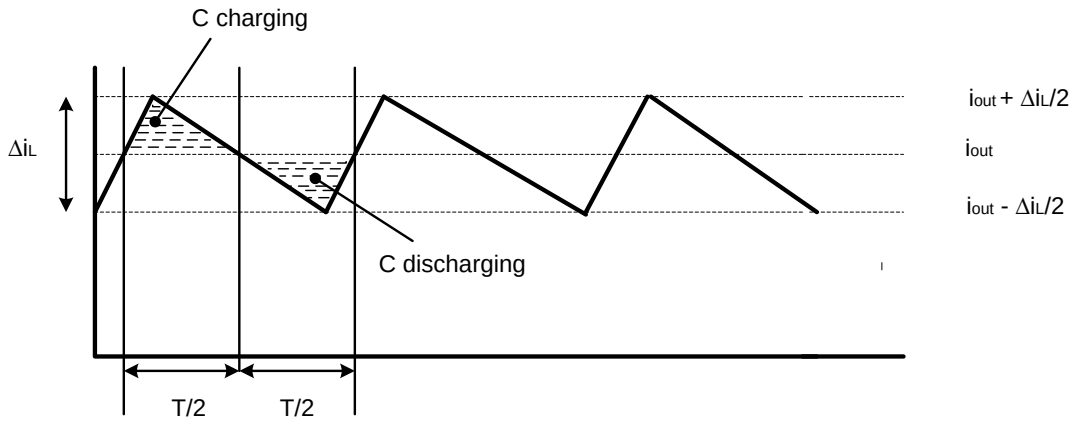

Figure 3-13: Inductor Current Waveforms used to Illustrate Capacitor Charging

And from 3.20, we have:

$$\Delta V = \frac{\Delta Q}{C} = \frac{1}{C} \times \frac{1}{2} \times \frac{T}{2} \times \frac{\Delta i_L}{2} = \frac{T \times \Delta i_L}{8 \times C} \tag{3.26}$$

In the worst case, $\Delta i_L = 2 \times i_{out}$ and therefore,

$$C_2 = \frac{i_{out}}{4 \times \Delta V \times f_{PWM}} \tag{3.27}$$

Where i_{out} is the converter output current at maximum input power, ΔV is the voltage ripple and f_{PWM} is the switching frequency.

3.5.2. Maximum Power Point Tracking

A Maximum Power Point Tracker (MPPT) is an electronic DC/DC converter that optimizes the match between the PV module and the load: The main function of Maximum Power Point trackers is to maximize the PV module output power despite of the ambient temperature and insulation levels.

As seen in the I-V curve of typical PV modules (Figure 3.2) there exists a single point at that point the power is maximum [16]. It means that there is a peak power corresponding to a particular voltage and current [16]. As the efficiency of the solar panel is low it is desirable to operate the module at the peak power point so that the maximum power can be delivered to the load [16].

There are several studies of MPPT techniques, such as the perturbation and observation, the constant current method, the constant voltage method and the incremental conductance method [16]. The next subchapter will focus on the constant voltage method (algorithm implemented to track MPPT).

3.5.2.1. Maximum Power Point Method

Since the I-V characteristics of a PV cell is non-linear, maximum power point can be different for each irradiance condition on the solar cell [16]. To fit the demand of a low power algorithm, a simplified 75% constant voltage method was used to deduce the maximum power point [16]. Instead of finding the maximum via derivative, and employ numerical methods to show a linear dependency between "cell voltages correspond to maximum power" and "cell open circuit voltages" thus it is assumed that a maximum power point of the used solar PV module lies at about 0.75 times (MV value – voltage factor) the open circuit voltage of the module: the MPPT can be found at 75% of the open circuit voltage [16].

Therefore, by measuring the open circuit voltage of the solar panel, V_{OC}, from equation 3.24 a reference voltage can be generated (V_{MP}) and a duty cycle control scheme can be implemented in order to bring the solar PV module voltage to the point of maximum power [16].

$$V_{MP} = M_V \, X \, V_{OC} \tag{3.24}$$

Although very simple this method has a low efficiency compared to other MPPT methods: in reality M_V is not constant and is affected by temperature and irradiance levels as already said above. Another limitation of this technique is the open circuit voltage of

the module: it varies with the temperature. Therefore, as the temperature increases the module open circuit voltage changes and it is required to measure the open circuit voltage of the module very often.

3.6.Battery

The demand for portable devices like, mobile phones, portable DVD players, PDAs, etc has grown tremendously during last decade, due to its integrated functionality and shrinking form factors. Of all rechargeable batteries available, Lithium-ion (Li-ion) battery has been widely adopted.

Li-ion batteries have several advantages over other rechargeable batteries, such as:

- The energy density is higher than most of the other rechargeable batteries. Therefore for the same size or weight they can store more energy than other rechargeable batteries.
- The operating voltage of these batteries is higher, typically about 3.7V for lithium-ion vs.1.2V for NiMH or NiCd. Thus saving on the number of cells used.
- The self discharge rate for the Li-ion batteries is lower than other types of rechargeable batteries.

Nevertheless Li-ion batteries have some disadvantages compared to others, such as:

- The cost of Li-ion batteries is much higher than similar capacity of NiMH or NiCd batteries. As these batteries are much more complex to manufacture.

- The Li-ion batteries also require sophisticated chargers that can carefully monitor the charge process.

In summary, the Li-ion batteries are smaller and lighter, have a higher voltage and hold a charge much longer than other types of batteries. For these main reasons, the Li-ion battery is chosen for the proposed solar charger.

With accurate and efficient circuit and battery model, it is possible to predict an intuitive and comprehensive electrical battery model. The next subchapter deals with the model of a Li-ion battery that is suitable to test the behavior of portable battery powered systems. The electric model is built by a combination of voltage sources, resistances and conductors.

3.7. The DC to AC Inverter

The DC to AC voltage converter ties the DC output of the MPPT with the AC bus of the utility grid. Most grid tie PCU's use self-commutated voltage source inverters which are built with switching devices such as IGBT's or MOSFET's. These types of switches have the advantage of allowing control of both the on and off switching events. This characteristic is optimal for normal DC to AC inverter operations and in addition allows for the existing switches of the inverter to be used for protection functions. Thus the self-commutated inverter can provide control of the power factor and suppression of harmonic current, as well as protection against grid disturbance.

The goal of this work is to study the affect PV generators will have on the utility distribution grid. PV generators are often single phase devices which produce power at low voltage levels. These characteristics match well with distribution systems which allow for single and two phase feeders and distribute power at mid to low voltage levels, therefore a majority of PV generation systems are connected to the distribution system.

In this thesis, a real distribution system with PV cluster given in [10] has been simulated. The network configuration is shown in figure 24. The low-voltage (11.4KV) distribution system is connected to the high-voltage distribution system through a 3-phase transformer T1 (25MVA, 69KV/11.4KV), and the PV generator is connected at one of the feeder of the distribution lines which is in turn connected to the distribution substation in the residential area through a pole mounted transformer T2 (1ϕ , 167kVA, 6.58kV/220V), which transforms the voltage from 6.58KV to 220V. The actual data for transformer, line impedance, and load in this demonstration system are listed in Table 1-3 respectively. This particular site is chosen because it has the largest PV capacity in Taiwan residence until now. The SIMULINK block diagram of the above mentioned real distribution system with PV generator connected at bus 7 is shown in Figure 16. Figure 17 shows the PV generator sub-system it takes into consideration cell's open circuit voltage, cell's temperature and solar irradiance to calculate the output current and power. This PV generator block is a flexible one by varying the number of modules connected in series and parallel one can achieve desired voltage, current and eventually power. In figure 3.14 MPPT sub-system is shown.

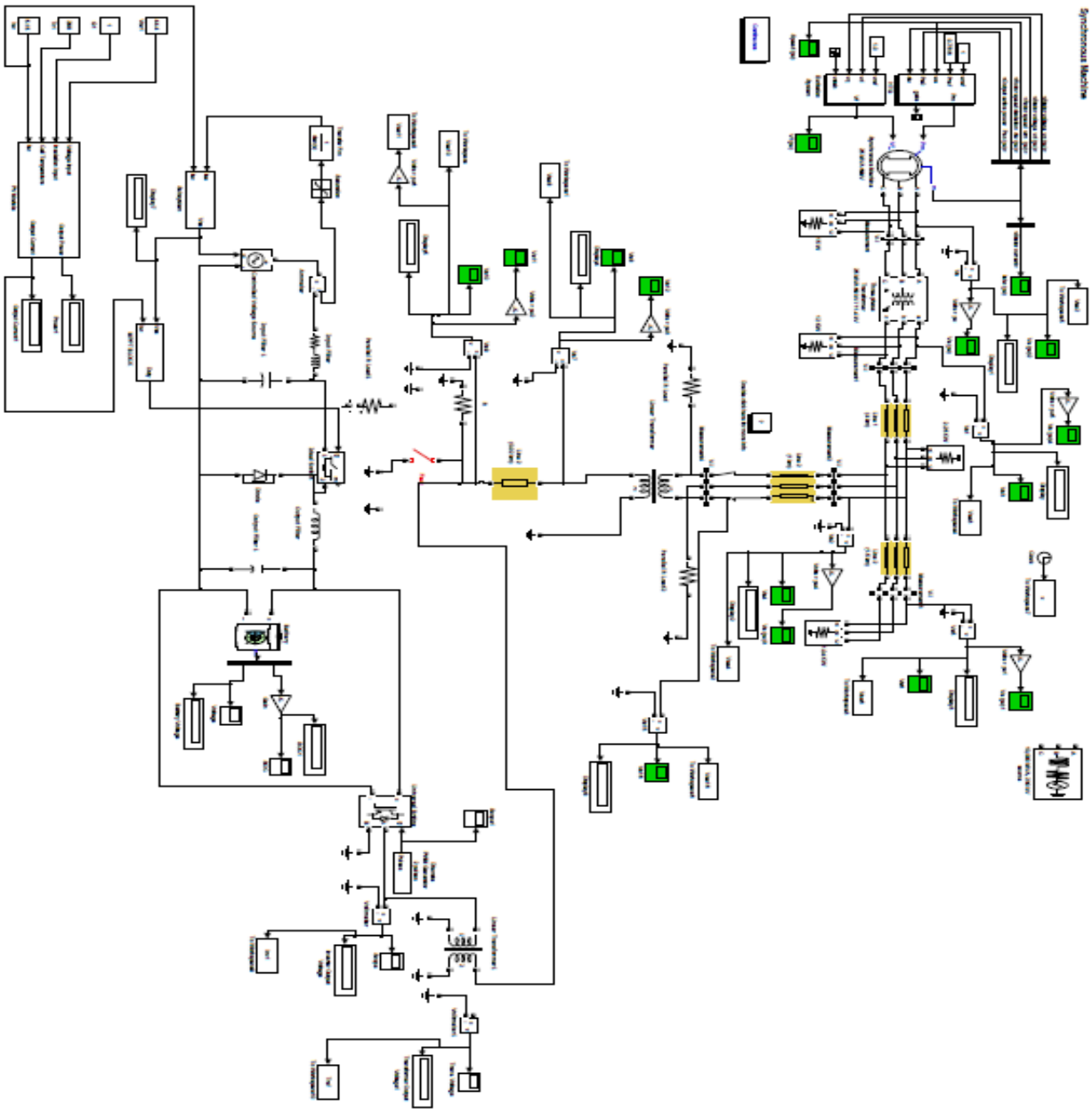

Figure 3-14: Simulink block diagram of the PV generator integrated with Utility System

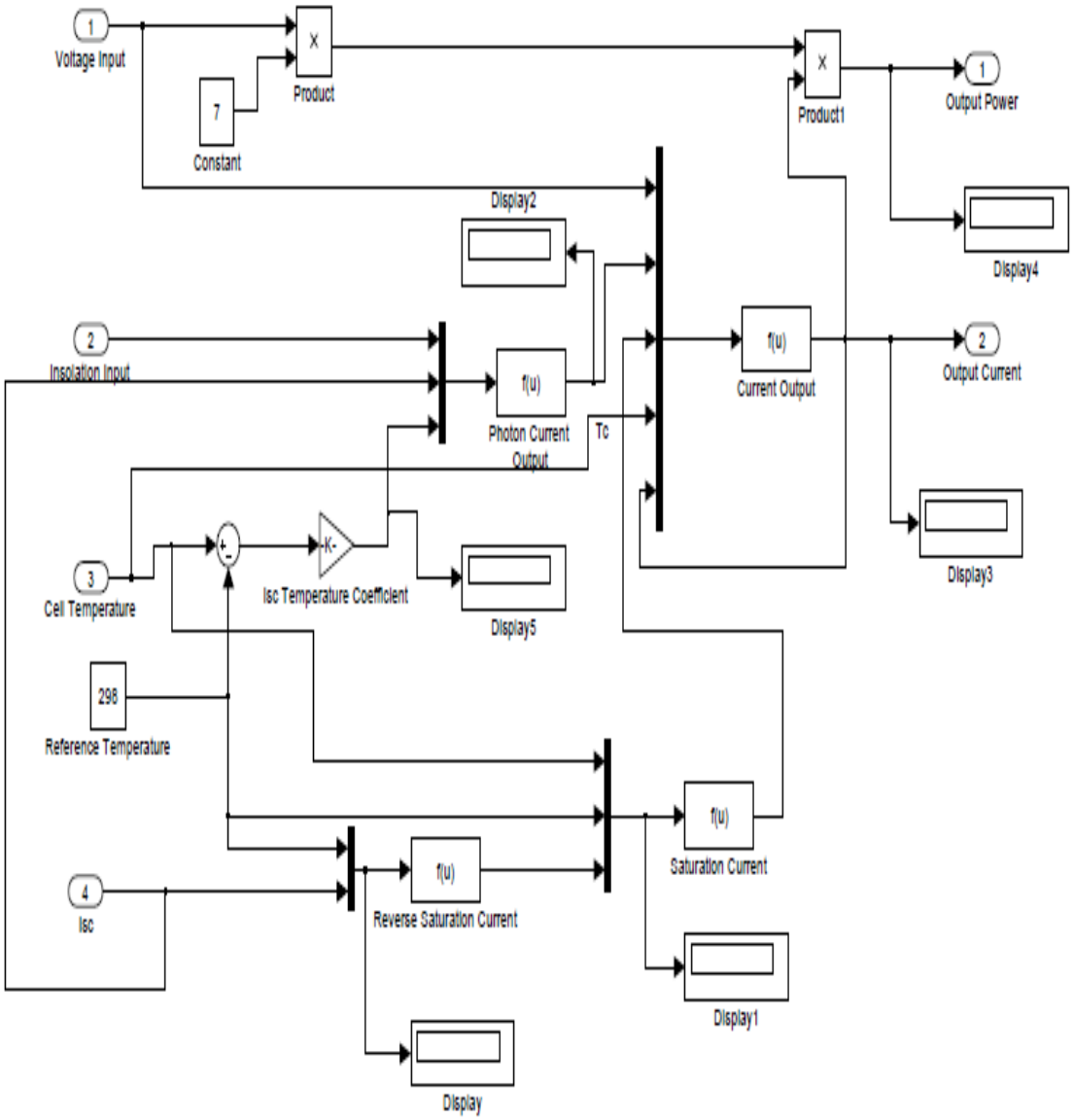

Figure 3-15: PV generator sub-system

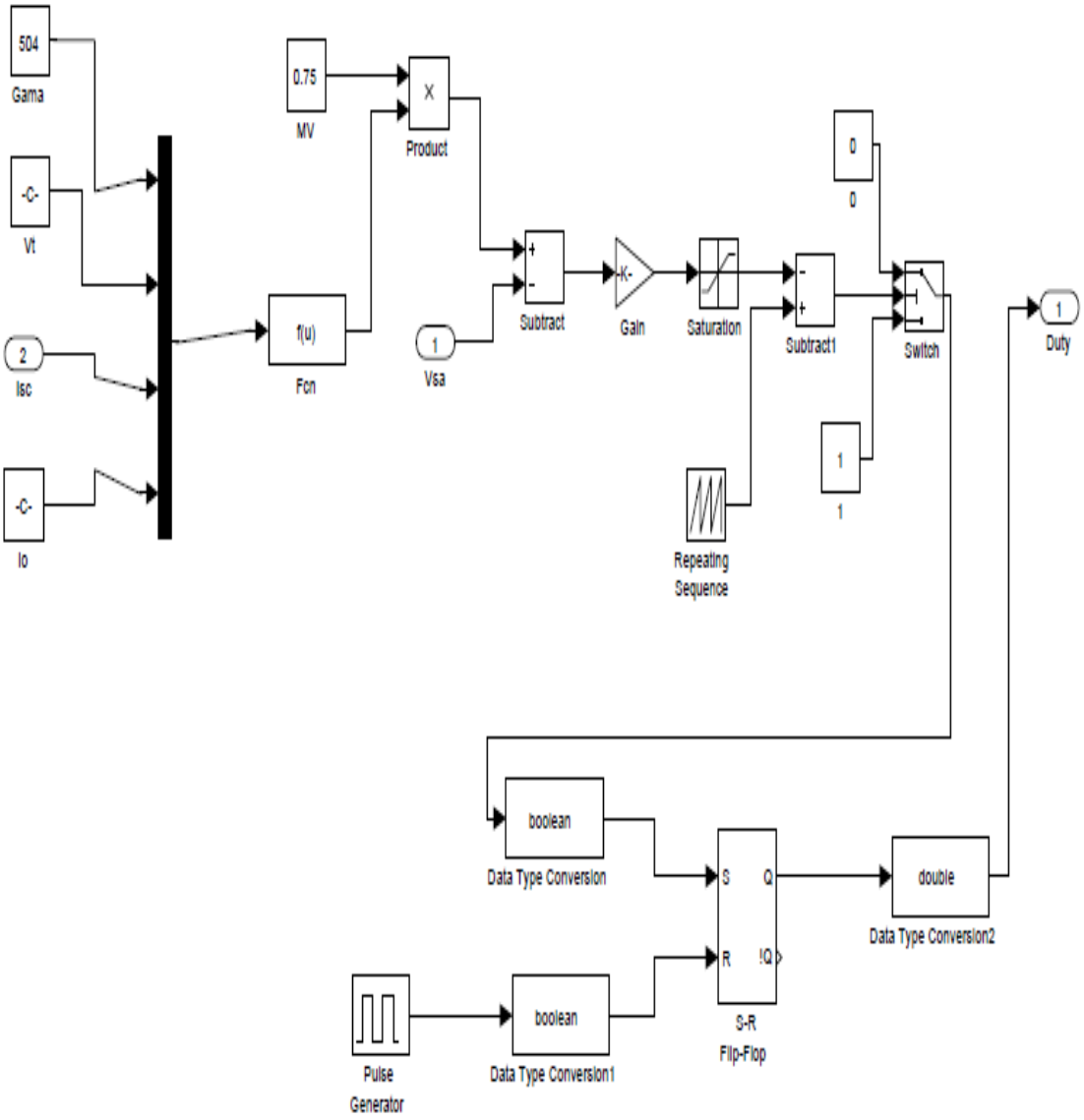

Figure 3-16: MPPT block sub-system

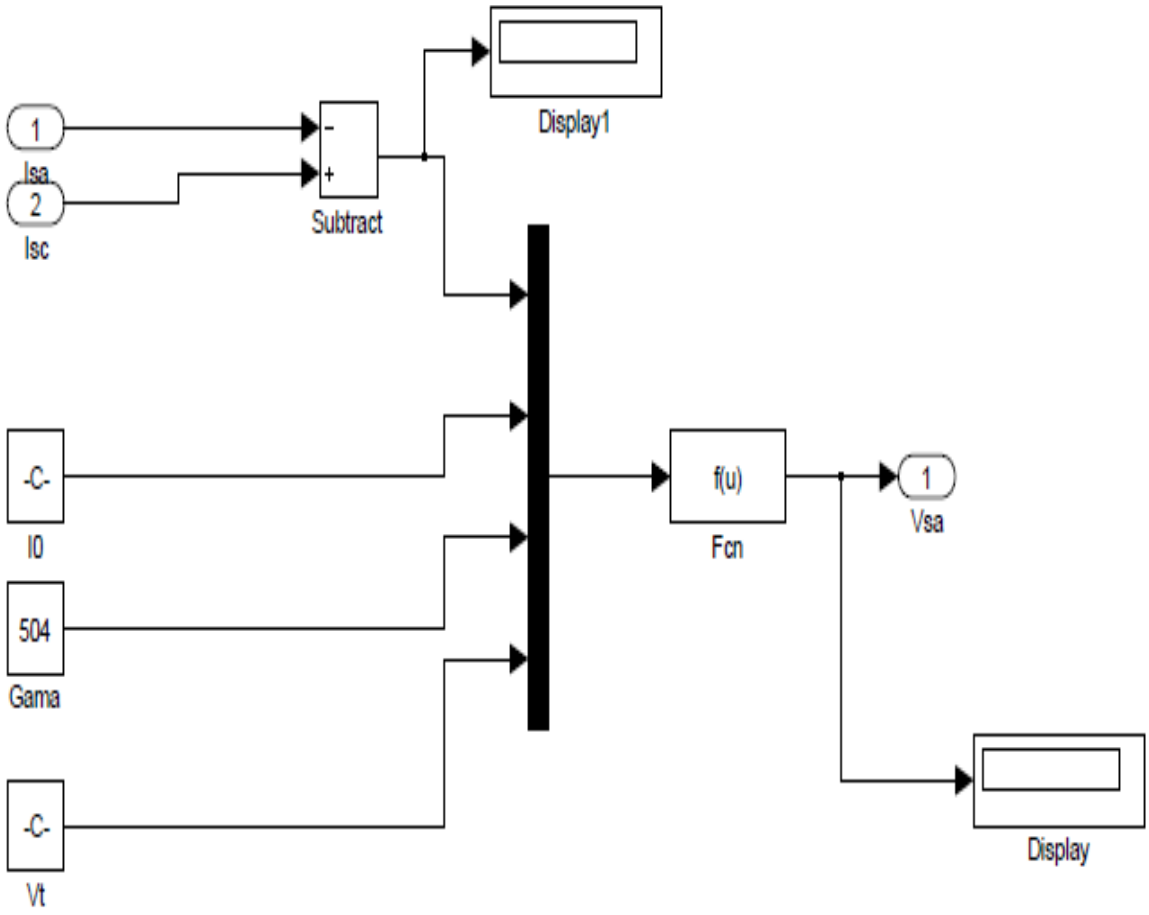

Figure 3-17: Determination of open circuit voltage subsystem

Transformer	S (KVA)	X_{pu} (%)	X/R	Rated V	R (Ω)	R(Ω)	L(H)	L (H)
T1	25000	9.31	20	3ϕ, 69KV/11.4KV	0.866	0.0242	0.047	0.00128
T2	167	2.17	5	1ϕ, 6.58KV/220V	1.103	0.0146	0.0123	1.636 x 10^{-5}

Table 3-1: Transformer data summary

Impedance	Type	Length (KM)	Rated V	R(Ω/KM)	X(Ω/KM)
Z1	3C500XP2	4	11.4KV	0.1075	0.1437
Z2	3C500XP2	1.5	11.4KV	0.1075	0.1437
Z3	3C#1XP2	1	11.4KV	0.5426	0.1896
Z4	3C#1XP2	0.02	220V	0.3325	0.0977

Table 3-2: Line impedance summary

Load	L1	L2	L3	L4
Peak load (KVA)	12.94	2.5	1.16	75
Light load (KVA)	4	1.37	0.63	15

Table 3-3: Load data Summary

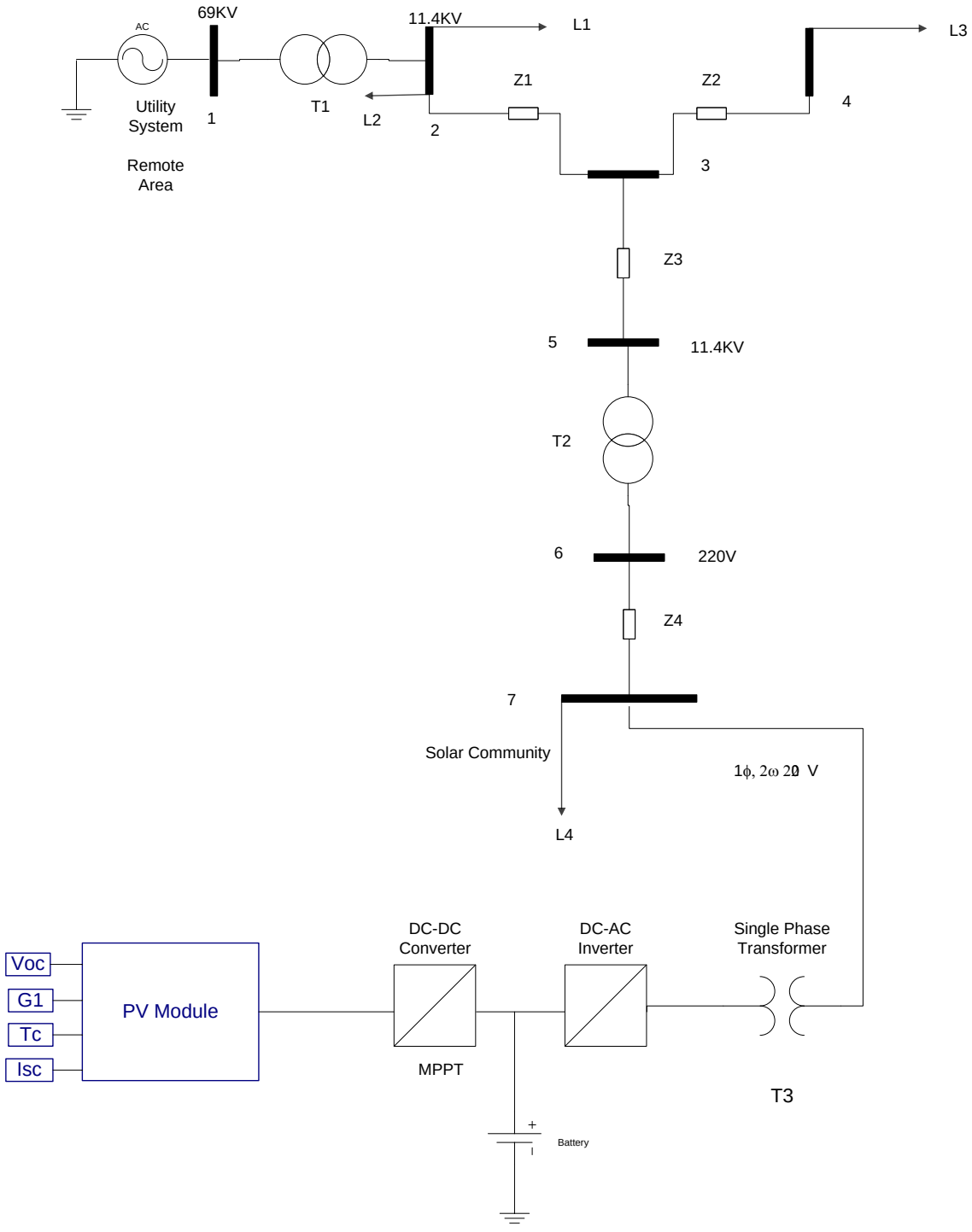

Figure 3-18: Single Line Diagram of solar charger

CHAPTER 4

4.Results and Discussion

In this chapter the results obtained from the SIMULINK model of a real distribution system to which PV array is integrated at the load bus are presented. At first, PV array's V-I and P-V characteristics are compared with that of manufacturer's data. The nonlinear nature of PV cell is obvious, i.e., the output power and current of Photovoltaic cell depend on the cell's terminal operating voltage and temperature, and solar irradiance as well [11]. From Figs. 4.1 and 4.2 it is clear that with increase of solar insolation, the short-circuit current of the Photovoltaic array increases, and the maximum power output increases [11]. This is because, the open-circuit voltage is logarithmically dependent on the solar irradiance, yet the short-circuit current is directly proportional to the radiant intensity [11]. In Figure 4.1 and 4.2 I-V and P-V characteristics are plotted for different solar irradiance levels from G=1 to G=0.25, if G=1 it means that solar panel is receiving solar energy at the rate of 1000 W/m2. As the value of 'G' drops, thus the net energy received by the solar panel also drops. It is important to note that the developed module's outputs that are current and power depend on the irradiance and cell's temperature [11]. Moreover , we can spot that in Figs. 4.3 and 4.4 it is clear that with increase of working temperature, the short-circuit current of the PV cell increases, whereas the maximum power output decreases. This is because, the increase in the output current is much less than the decrease in the voltage, thus the net power decreases at high temperatures [11].

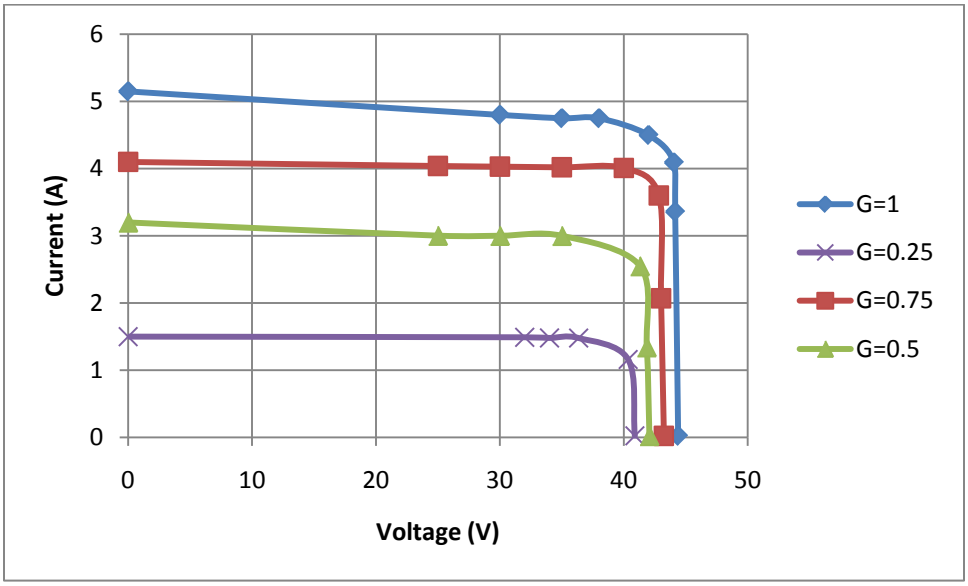

Figure 4-1: V-I Characteristics at different values of solar irradiance

Figure 4.1 presents V-I characteristic of the Suntech Power STP170S-24/Ac Solar panel the one used in this thesis. From the Figure we can deduce that the chosen voltage factor for the MPPT tracking validates the solar panel. The maximum power point (looking at V-I characteristic) can be found at approximately 75% of the open circuit voltage. By this, it is clear that the chosen M_V =0.75 is a good approximation.

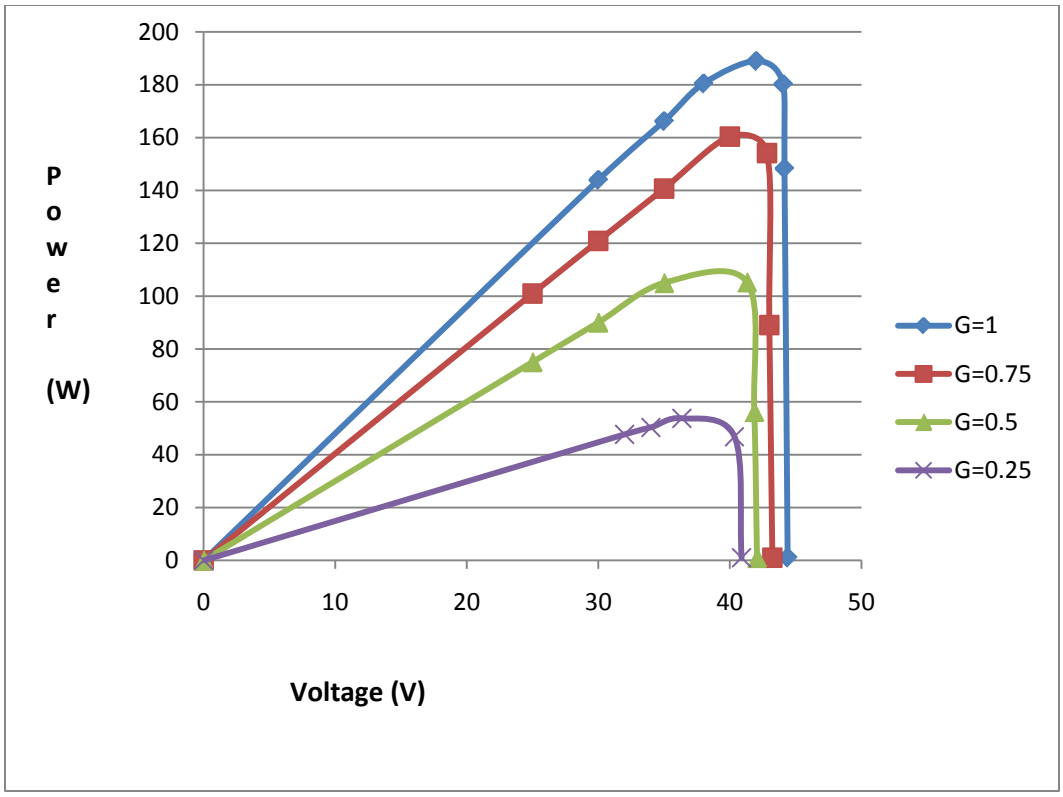

Figure 4-2: P-V Characteristics at different values of solar irradiance G=1=1000W/m2.

By analyzing P-V characteristic it is possible to comment that the solar panel modulation in SIMULINK environment is reliable. The maximum output power for the solar panel (according to available elements from the PV datasheet) respects the maximum operating point achieved.)

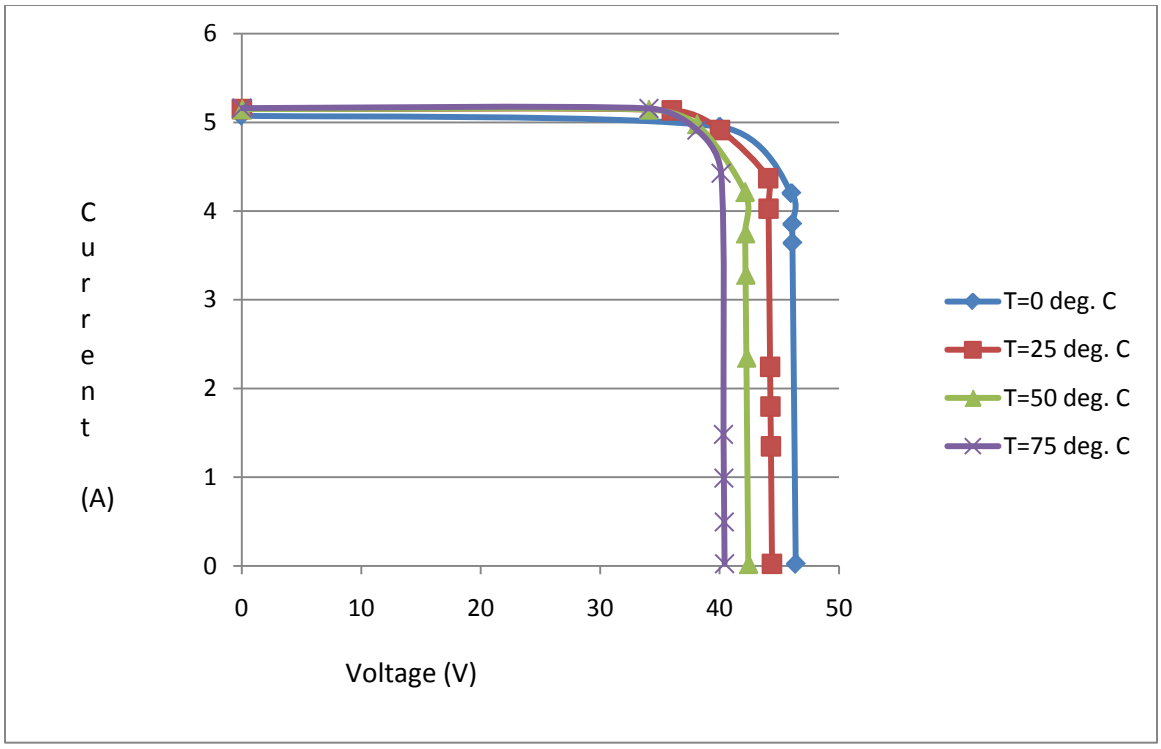

Figure 4-3: I-V Characteristics at different values of cell's temperature

In Figure 4.3 V-I characteristics are plotted for different values of cell's temperature and it is clear from the plot that as the temperature increases no doubt short-circuit current increases by a small value but at the same time the drop in open-circuit is high. Thus, the net power generated will drop.

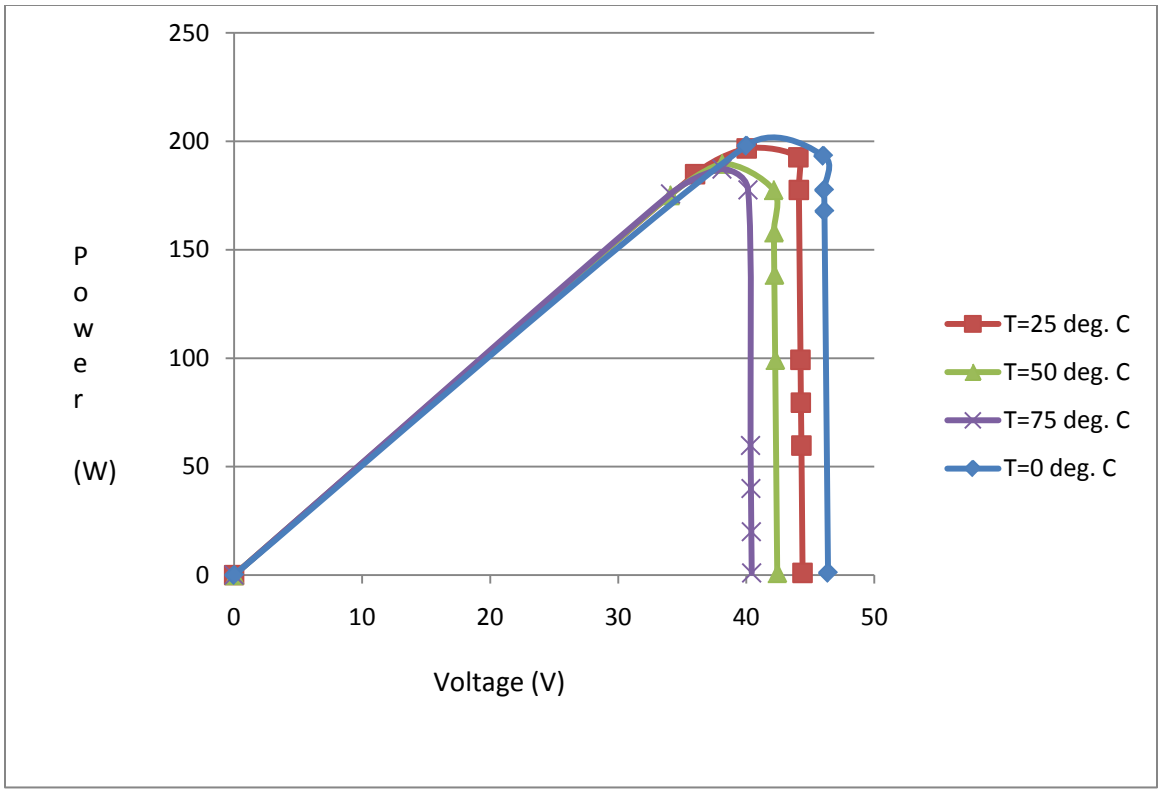

Figure 4-4: P-V Characteristics at different values of cell's temperature

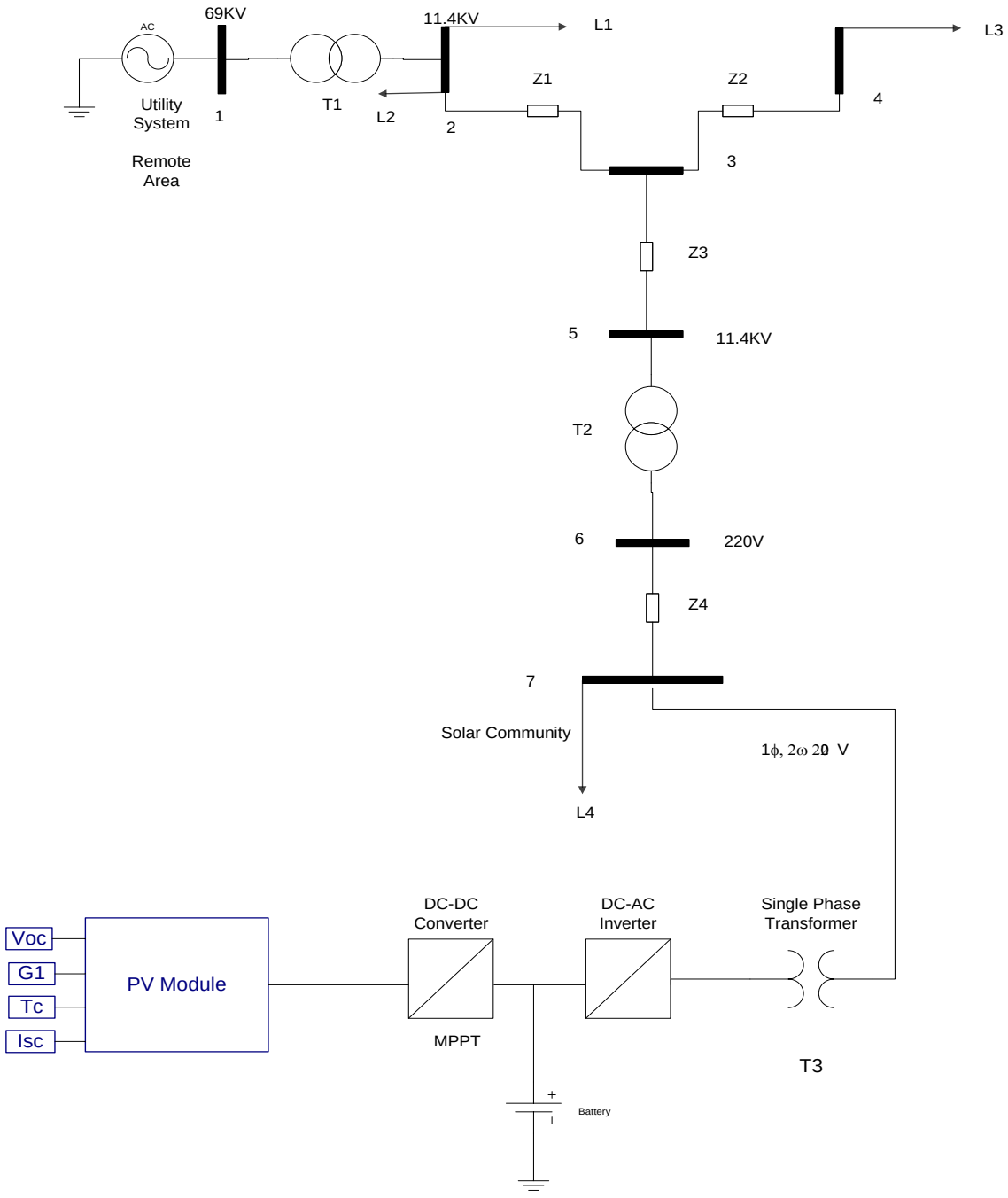

Figure 4-5: Single Line Diagram of Solar Charger

Since a typical PV cell model that has been developed in SIMULINK produces less than 2W of power at 0.5V approximately the cells must be connected in series-parallel combination on a module to produce desired output power [11]. In one of the configuration seven modules are connected in series so that the output voltage of the PV generator be around 310V then this string of seven modules is connected with 19 other modules in parallel to generate the output power of 32KW, the developed model is shown in the Figure 4.5 and the above mentioned model is simulated in SIMULINK. The V-I and P-V characteristics at different temperatures and over the range of solar insolation (irradiance) values, of the PV array which generates the net output power of 32KW are shown in Figures 4.6, 4.7, 4.8 and 4.9, the DC power produce by the PV generator is inverted with the help of IGBT inverter, the inverter output voltage is shown in Figure 4.10, the AC output voltage obtained from the inverter is step-down to 220V (RMS) with the help of a single-phase transformer whose output is shown in Figure 4.11 the secondary of the transformer is integrated with the Utility. In order to study the system characteristic for PV connection, especially for grid voltage control, numerical simulations have been carried out in this work. The system circuit and associated parameters have been established to simulate the PV system connected to the Utility system. Based on the simulation results, if there are no installed PV panels, the grid voltages are 220V under light load conditions. When the PV panels are installed and PV generation produces maximum output power, then the grid voltage of the load bus will increase from 220V (without PV) to 223.2V (with PV).

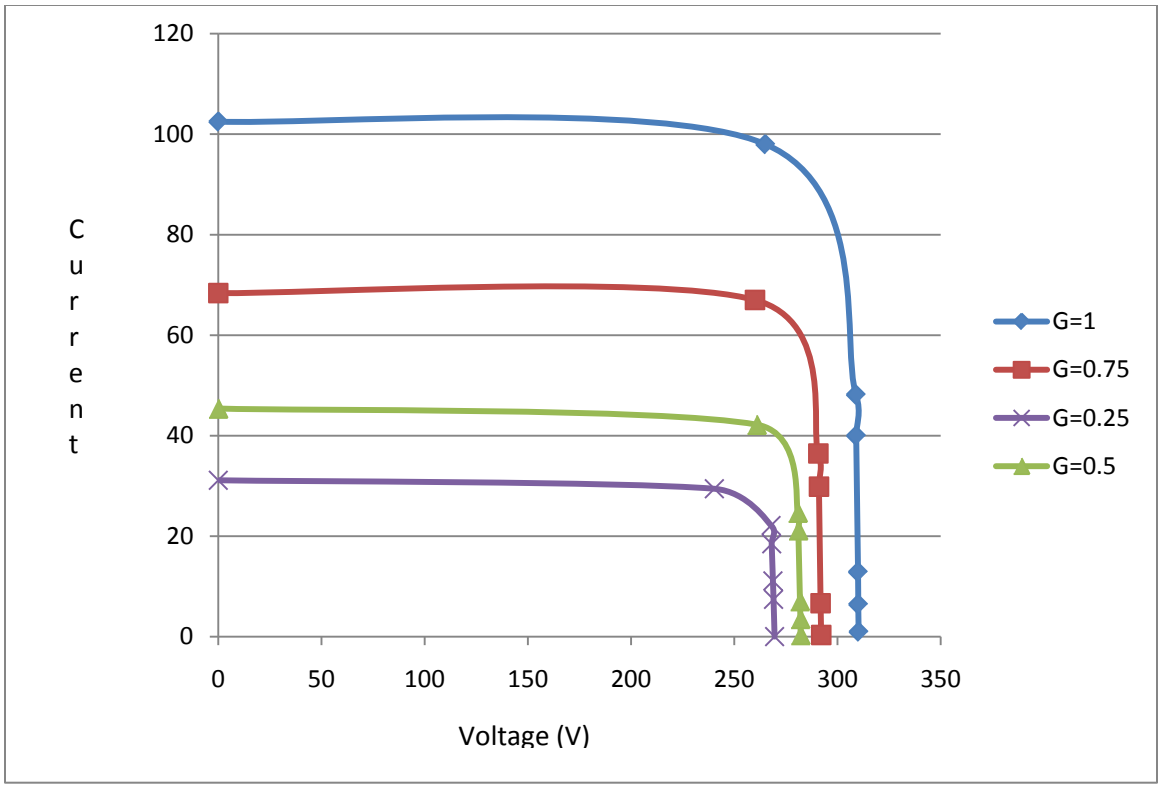

Figure 4-6: I-V Characteristics of a PV array generating 32KW power at different values of solar irradiance

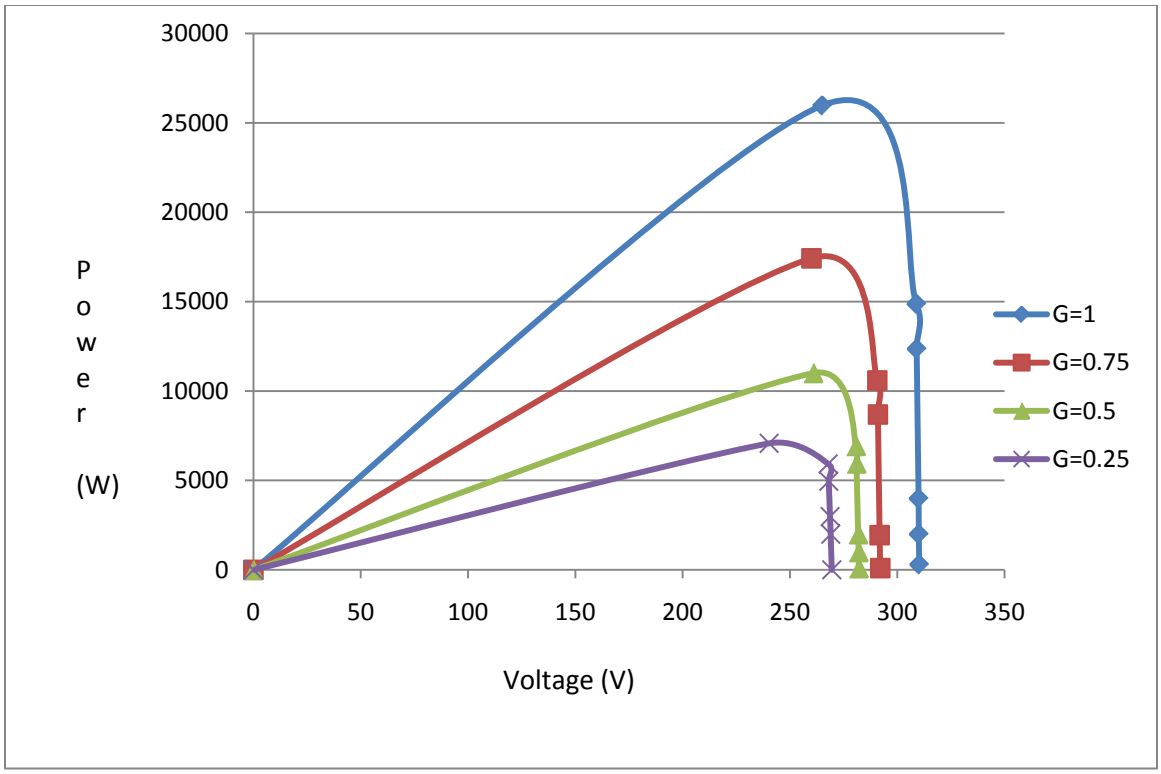

Figure 4-7: P-V Characteristics of a PV array generating 32KW power at different values of solar irradiance.

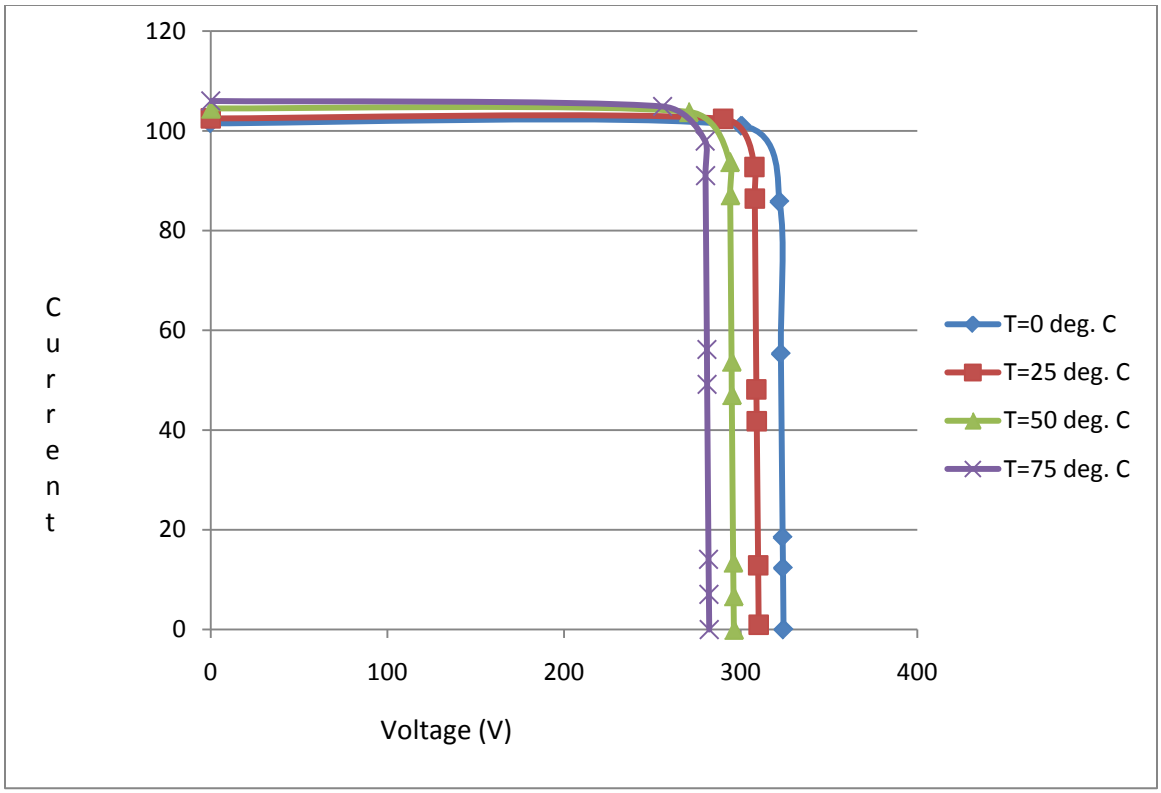

Figure 4-8: I-V Characteristics of a PV array generating 32KW power at different values cell's temperature.

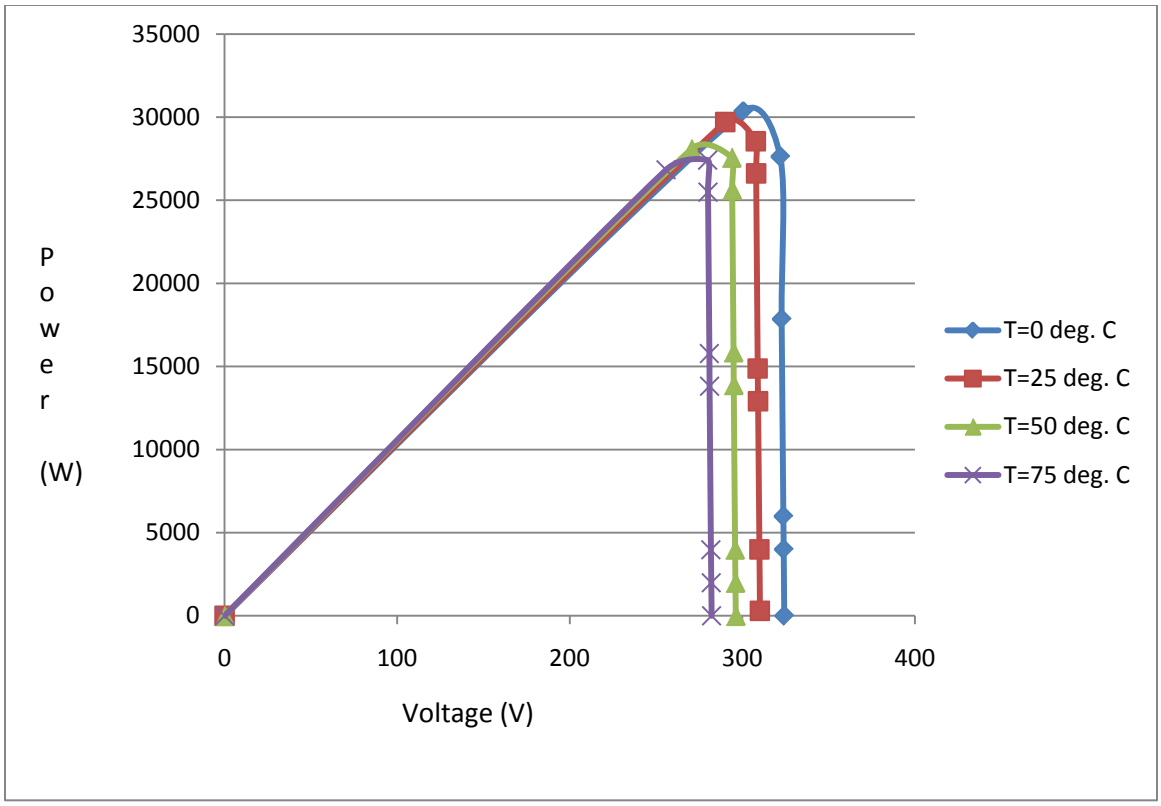

Figure 4-9: P-V Characteristics of a PV array generating 32KW power at different values cell's temperature.

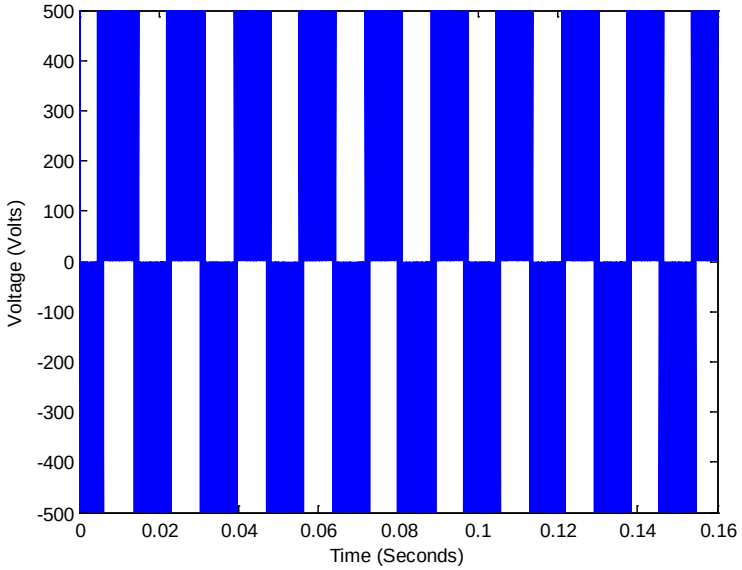

Figure 4-10: Inverter output voltage

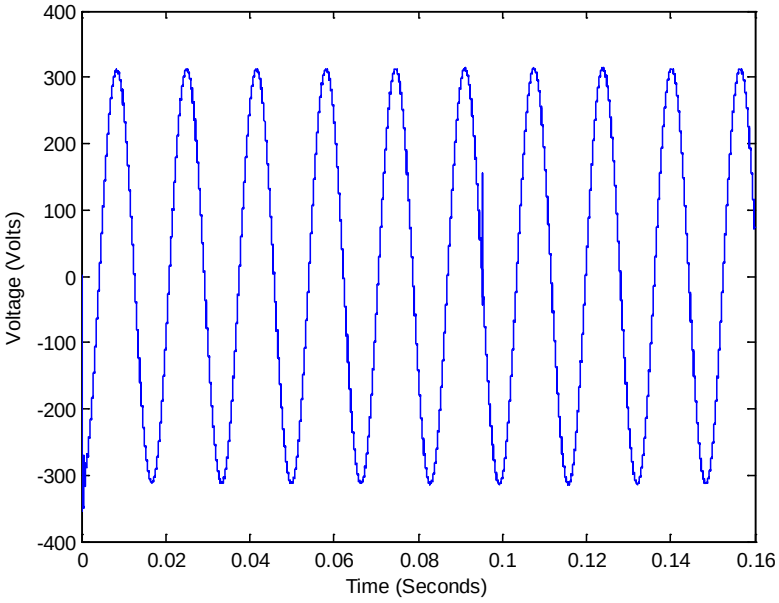

Figure 4-11: Transformer output voltage

4.1.PV cluster system steady-state simulation

In this thesis to study the steady-state characteristics of the system, especially for grid voltage control, when PV module is integrated at the seventh bus, numerical simulations have been carried out. In order to simulate the PV system, the system circuit and its associated parameters have been established in SIMULINK background. From the analysis of the simulation results it is clear that, if there are no installed PV panels, the grid voltages on the solar community are 220V under 75kVA consumer loads. In this work, 75kVA is assumed to be the peak load in total 15 houses of a community. When the PV panels are integrated and PV module produces maximum output power, then the grid voltage on loads will increase from 220V (without PV) to 223.2V (with PV).

In this PV integrated demonstration site, the voltage at the load bus is within the acceptable range (i.e. between 0.95 and 1.05pu) under all normal system conditions because the level of PV penetration is low and the distance between the substation and PV generator is short. However, to evaluate the effects of different levels of PV penetration on voltage rise a scenario analysis has been applied in this thesis. Table 4 shows the load flow results for the analyzed system with a scenario analysis. By analyzing the obtained results from the scenario analysis, a maximum of 60kW PV systems in this demonstration site can be connected along the 5 km long distribution system.

Bus	Base Case	Different Levels of PV Penetration					
	31.5KW	40KW	50KW	60KW	70KW	80KW	90KW
1	1.0	1.0	1.0	1.0	1.0	1.0	1.0
2	0.995	0.995	0.995	0.995	0.995	0.995	0.995
3	0.995	0.995	0.995	0.995	0.995	0.995	0.995
4	0.995	0.995	0.995	0.995	0.995	0.995	0.995
5	0.995	0.995	0.995	0.995	0.995	0.995	0.995
6	1.0096	1.019	1.025	1.032	1.038	1.048	1.054
7	1.015	1.027	1.039	1.048	1.057	1.066	1.078
	Voltages at different busses (pu)						

Table 4-1: Change in voltage levels (pu) of seven busses for different levels of PV penetration

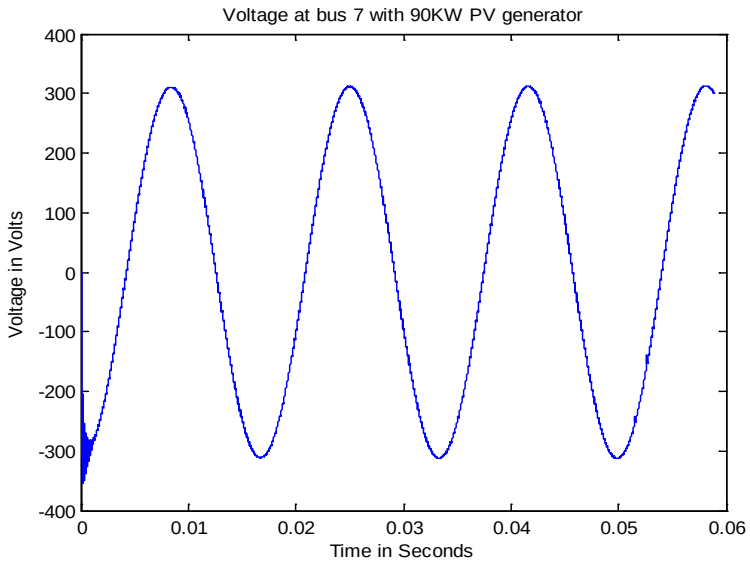

Figure 4-12: Voltage profile of bus 7 with 32KW of PV generator integrated at bus 7

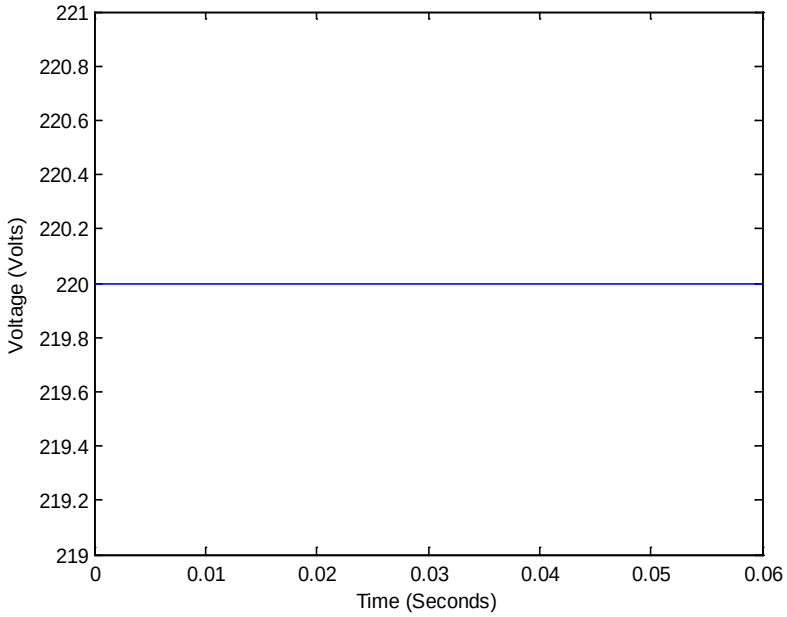

Figure 4-13: RMS voltage profile of bus 7 with 32KW of PV generator integrated at bus 7

4.2.PV cluster system fault analysis

Fault analysis is conducted on the developed system in order to analyze the system parameters, especially the voltage at the load bus. In this analysis at first, a three phase fault is applied for four and half cycles at the bus 5 and then a single phase fault is applied at bus 7, then its impact is studied at different busses. From the results obtained it was clear that, during fault the voltage of the busses drops from its steady-state value and when the fault is removed it returns to its original value.

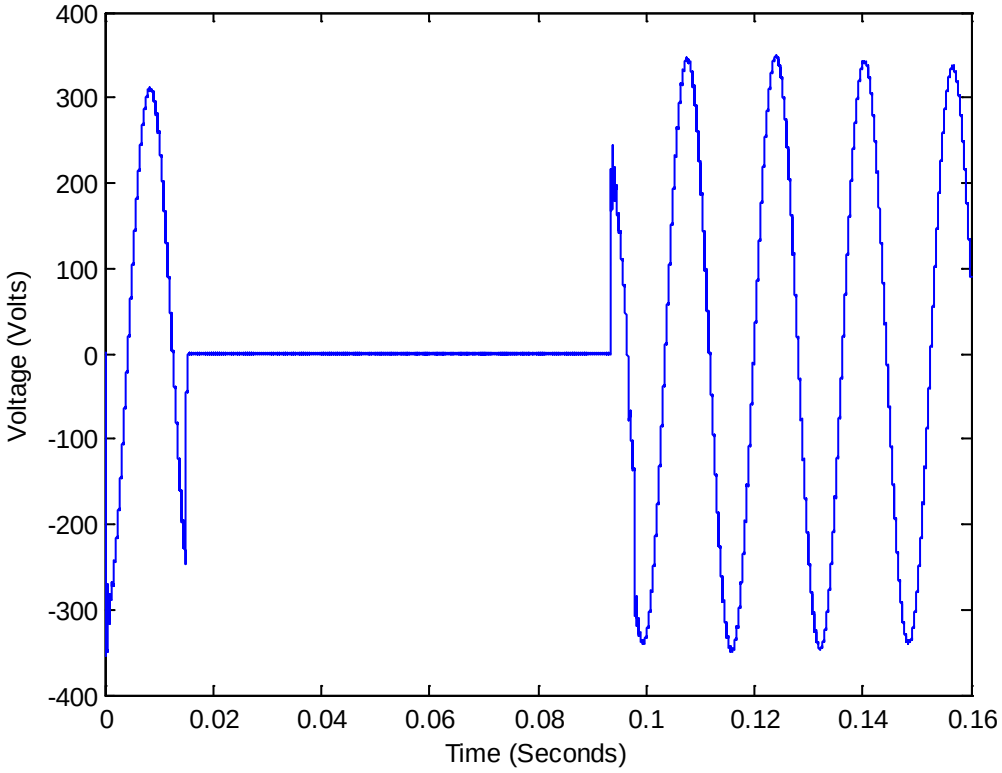

Figure 4-14: Voltage profile of bus 7 if a three phase fault occurred at bus 5 with 32KW PV generator connected at bus 7.

With the application of the three phase fault at the bus 5 the voltage at the bus 7 drops to zero during faulted period and when the fault is removed the voltage returns to the normal value. In the Figure 4.15 RMS plot of the Figure 4.14 is shown. Figure 4.16 till figure 4.21 voltage profile of the bus 6, 5, 4, 3, 2 and 1 is shown respectively. From these plots it can be stated that the voltage of the busses other than the faulted one drops to a particular value compare to the drop to a value of zero volt at the faulted bus, which is quite understandable.

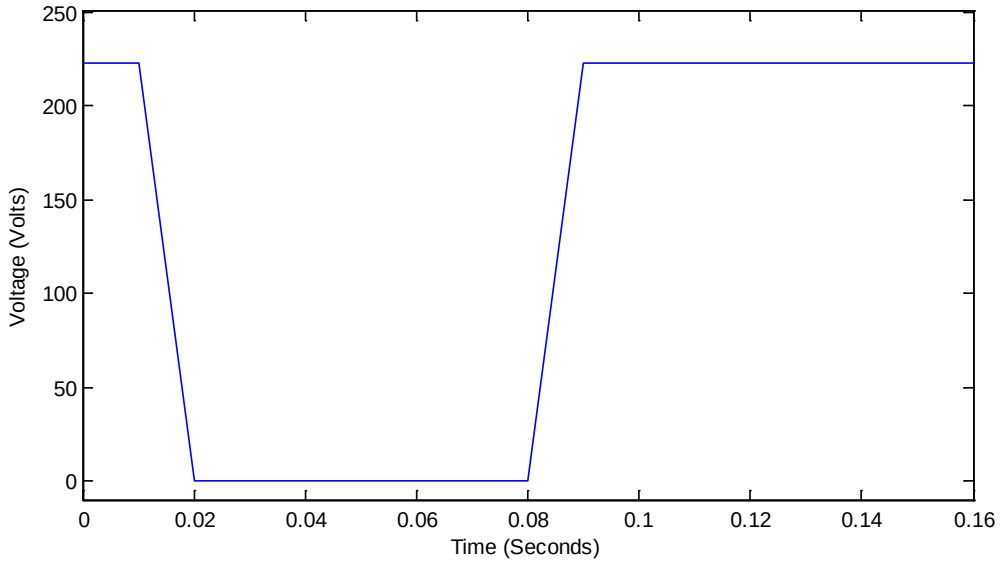

Figure 4-15: RMS value of the voltage at bus 7 if a three phase fault occurred at bus 5 with 32KW PV generator connected at bus 7.

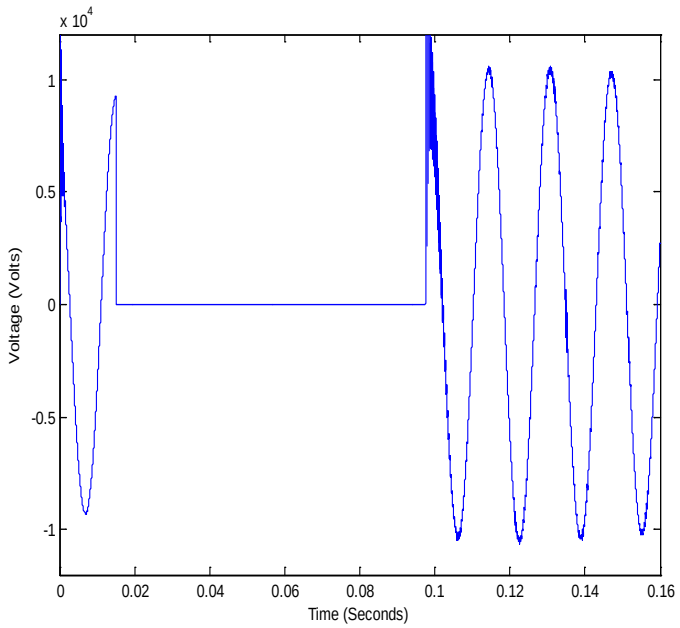

Figure 4-16: Voltage profile of bus 5 if a three phase fault occurred at bus 5 with 32KW PV generator connected at bus 7.

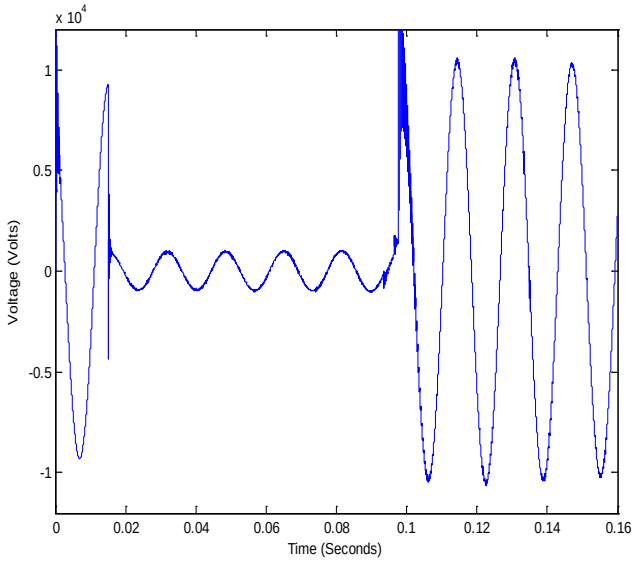

Figure 4-17: Voltage profile of bus 4 if a three phase fault occurred at bus 5 with 32KW PV generator connected at bus 7.

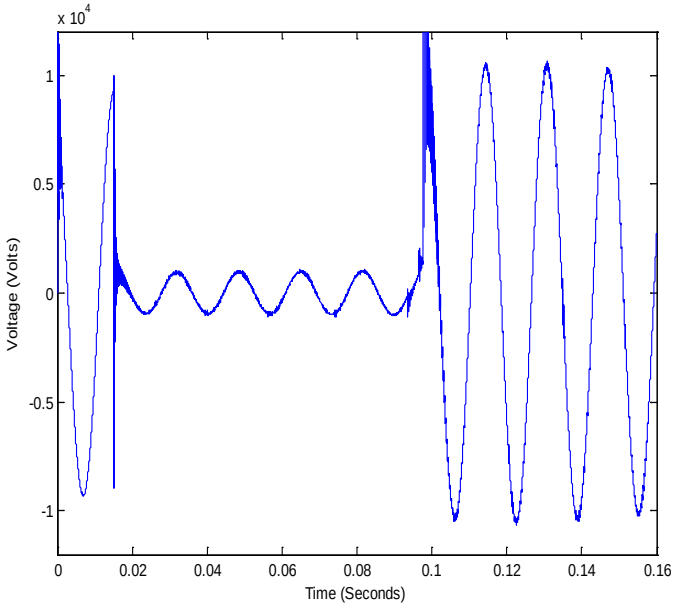

Figure 4-18: Voltage profile of bus 3 if a three phase fault occurred at bus 5 with 32KW PV generator connected at bus 7.

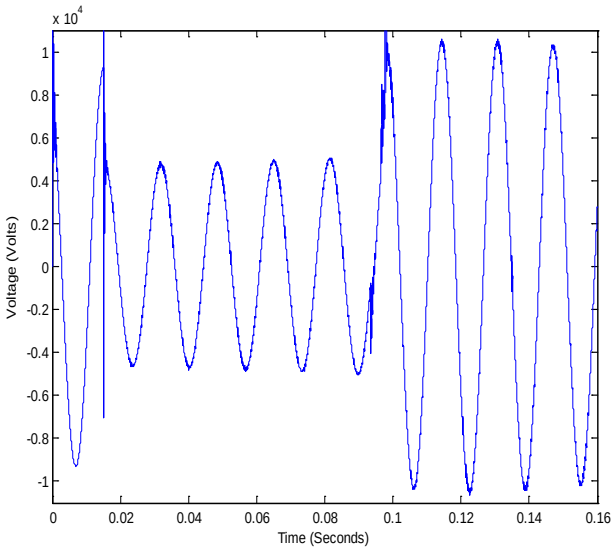

Figure 4-19: Voltage profile of bus 2 if a three phase fault occurred at bus 5 with 32KW PV generator connected at bus 7.

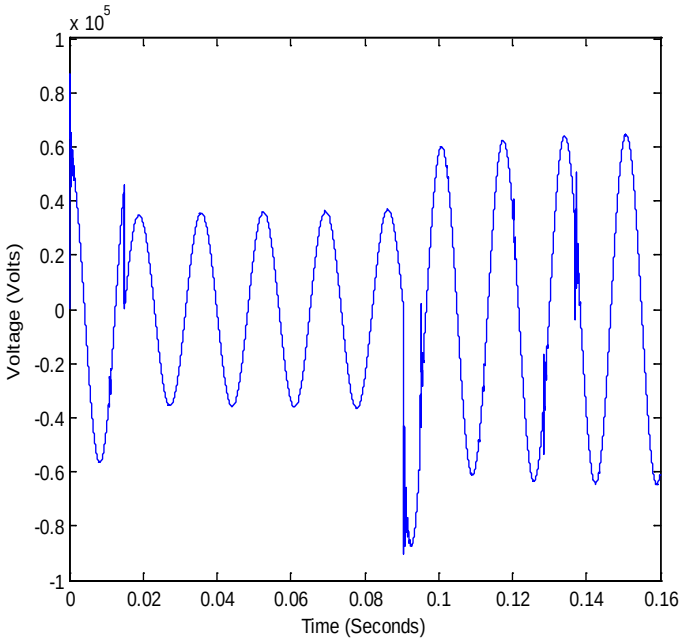

Figure 4-20: Voltage profile of bus 1 if a three phase fault occurred at bus 5 with 32KW PV generator connected at bus 7.

Voltage profile plots of the busses for the single phase fault occurred at bus 7

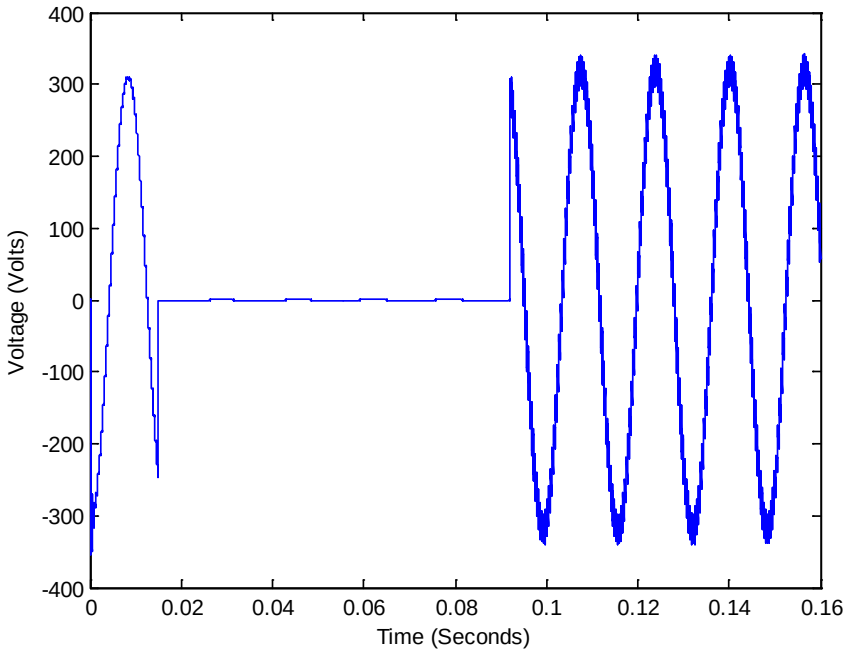

Figure 4-21: Voltage profile of bus 7 if a single phase fault occurred at bus 7 with 32KW PV generator connected to bus 7.

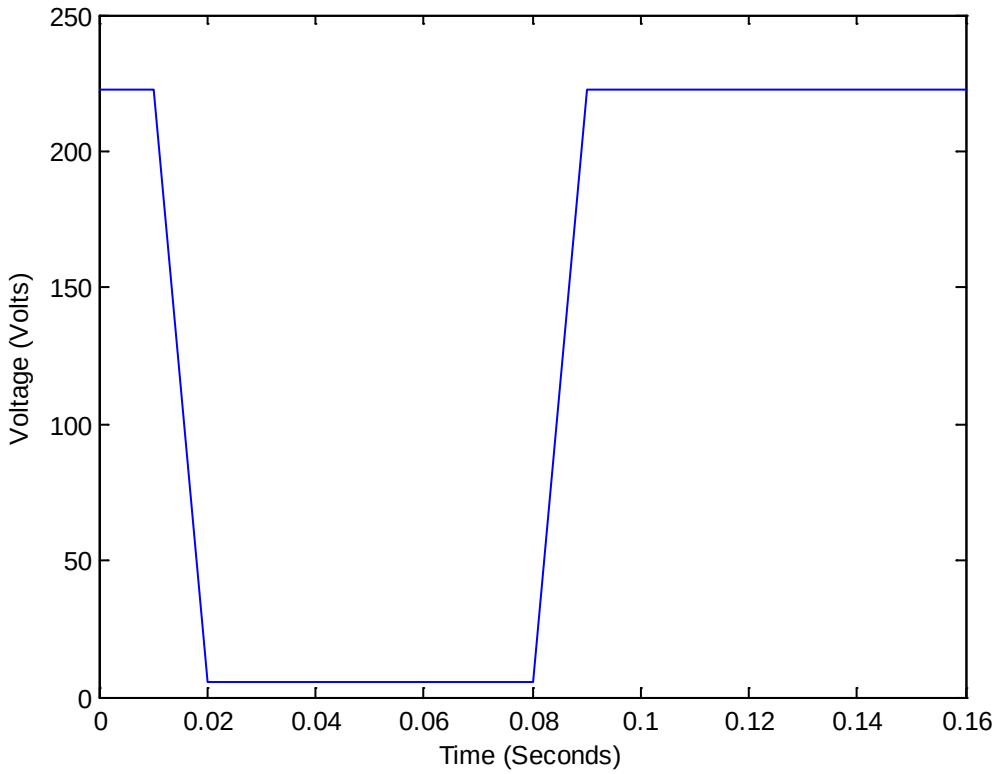

Figure 4-22: RMS value of the voltage at bus 7 if a single phase fault occurred at bus 7 with 32KW PV generator connected at bus 7.

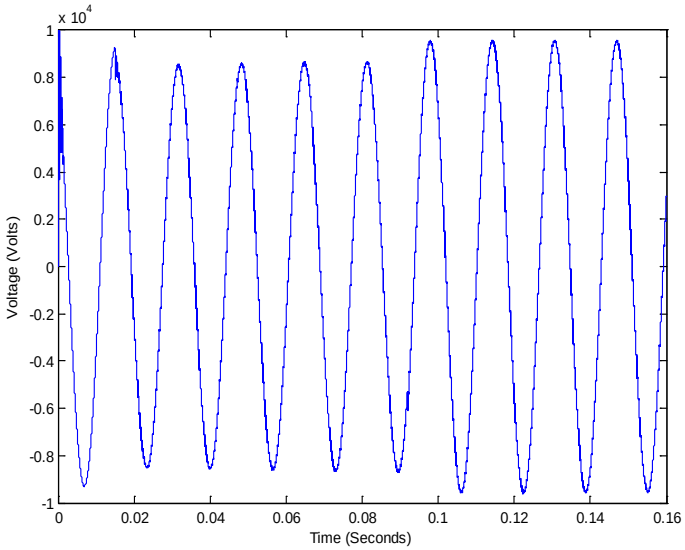

Figure 4-23: Voltage profile of bus 5 if a single phase fault occurred at bus 7 with 32KW PV generator connected to bus 7.

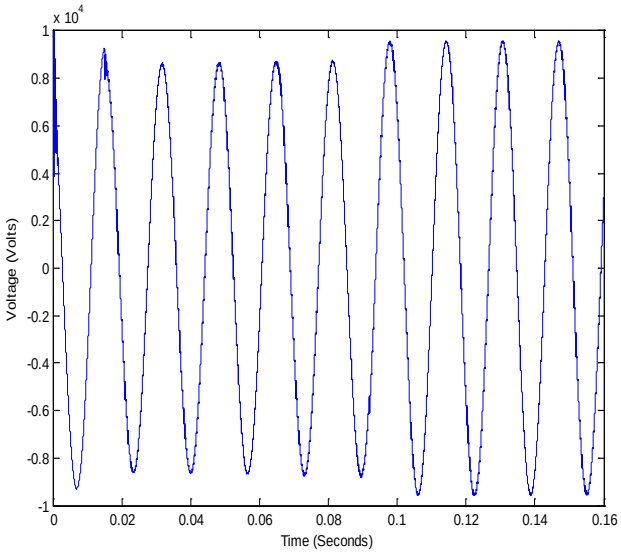

Figure 4-24: Voltage profile of bus 4 if a single phase fault occurred at bus 7 with 32KW PV generator connected to bus 7.

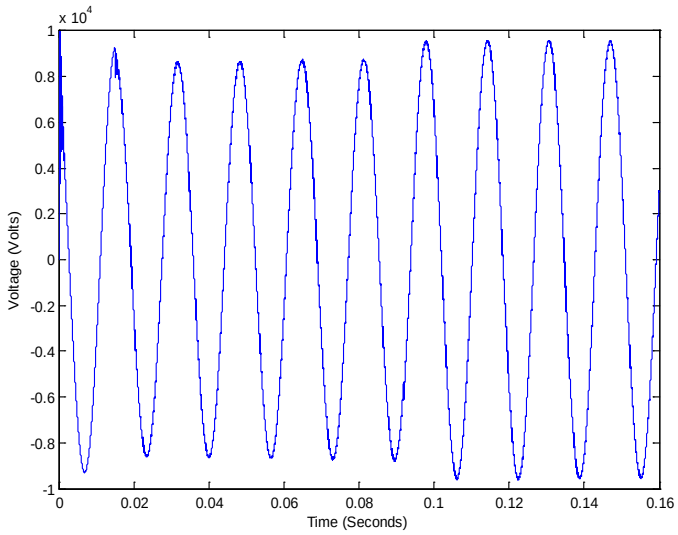

Figure 4-25: Voltage profile of bus 3 if a single phase fault occurred at bus 7 with 32KW PV generator connected to bus 7.

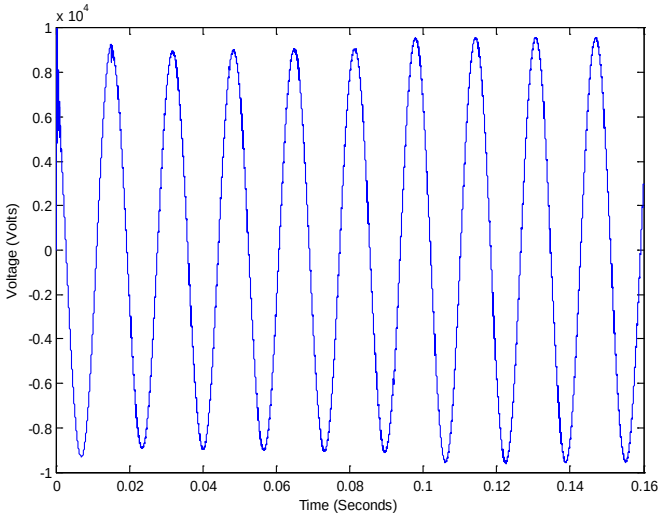

Figure 4-26: Voltage profile of bus 2 if a single phase fault occurred at bus 7 with 32KW PV generator connected to bus 7.

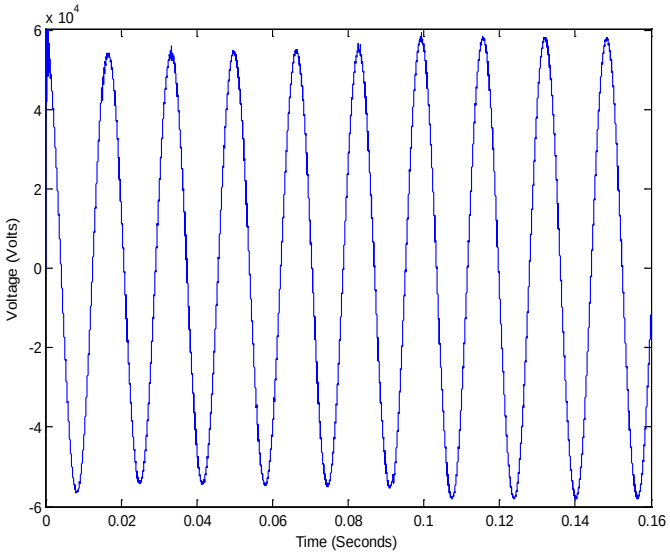

Figure 4-27: Voltage profile of bus 1 if a single phase fault occurred at bus 7 with 32KW PV generator connected to bus 7.

4.3. Fault analysis due to the fault occurred at the secondary of the transformer T3 of the PV generator or at the inverter output terminal

In this section, a single phase fault is applied at the secondary of the single phase transformer T3 which is connected to the point of common coupling between PV generator and Utility system; following results are obtained from the fault analysis.

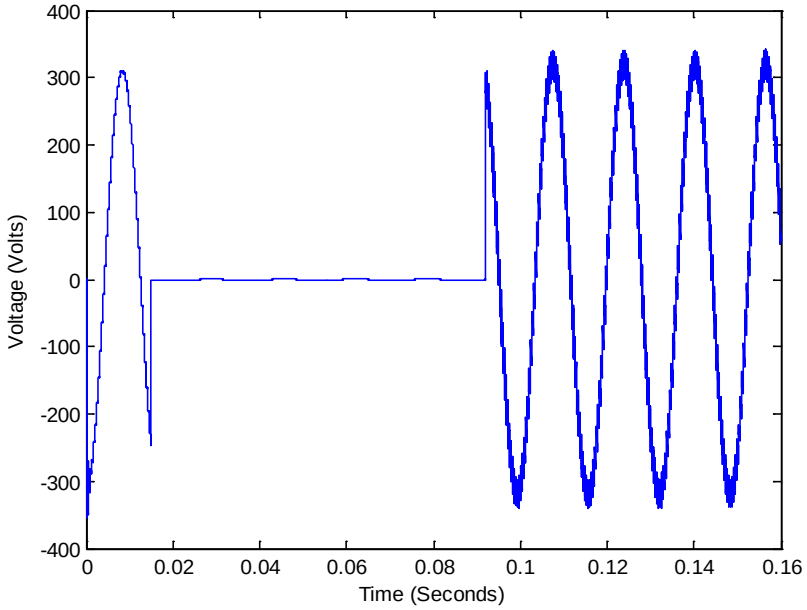

Figure 4-28: Voltage profile of bus 7 if a single phase fault occurred at the secondary of the transformer T3 with 32KW PV generator connected to bus 7.

From the above figure it is clear that by changing the position of fault from the point of common coupling (PCC) at bus 7 of distribution system to the secondary of the transformer T3 of the PV system the impact at the bus 7 on the voltage profile is similar.

Following figures shows the impact of the fault at different buses of the distribution system and the inverter output voltage plus the state of charge of the battery. In Figures 4.28-4.33 voltage profile of the busses 5, 4, 3, 2 and 1is shown respectively. From the analyses of the figures it can be stated that the impact of the fault at these busses is minimal, this is due to the distance of the fault and moreover these busses are fed from the source whose rating is very much higher in comparison with PV generator output power.

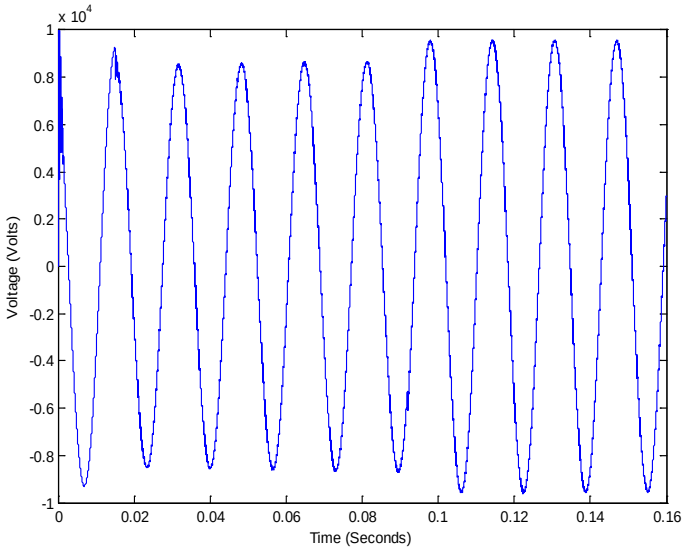

Figure 4-29: Voltage profile of bus 5 if a single phase fault occurred at the secondary of the transformer T3 with 32KW PV generator connected to bus 7.

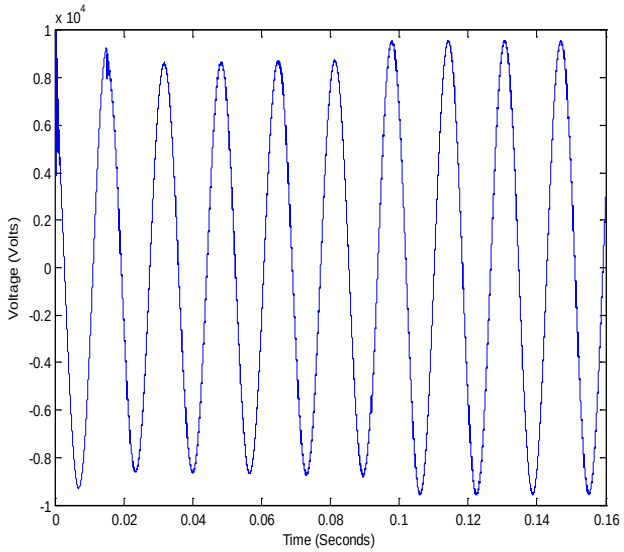

Figure 4-30: Voltage profile of bus 4 if a single phase fault occurred at the secondary of the transformer T3 with 32KW PV generator connected to bus 7.

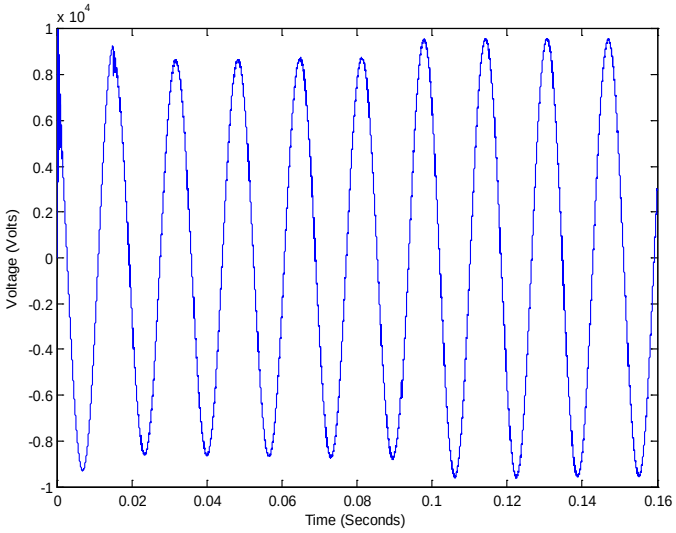

Figure 4-31: Voltage profile of bus 3 if a single phase fault occurred at the secondary of the transformer T3 with 32KW PV generator connected to bus 7.

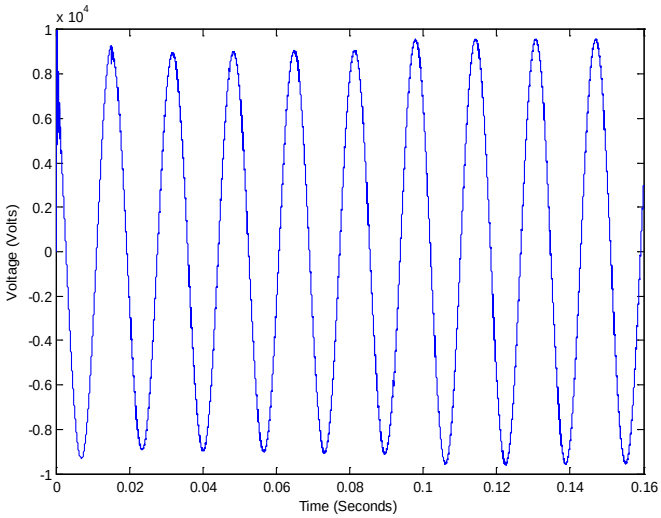

Figure 4-32: Voltage profile of bus 2 if a single phase fault occurred at the secondary of the transformer T3 with 32KW PV generator connected to bus 7.

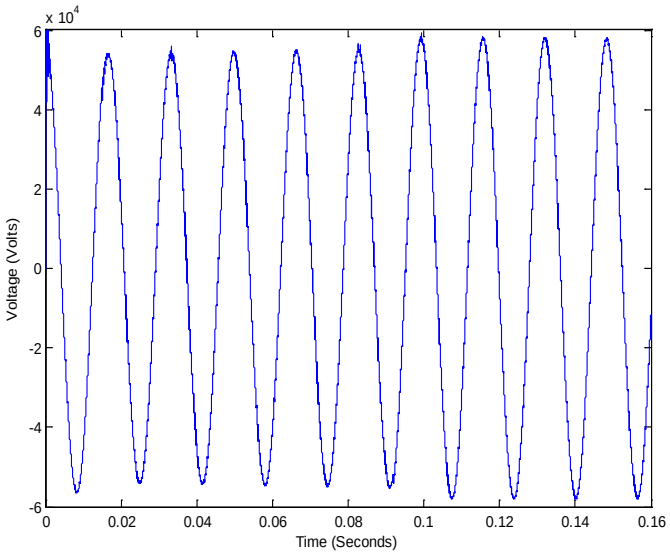

Figure 4-33: Voltage profile of bus 1 if a single phase fault occurred at the secondary of the transformer T3 with 32KW PV generator connected to bus 7.

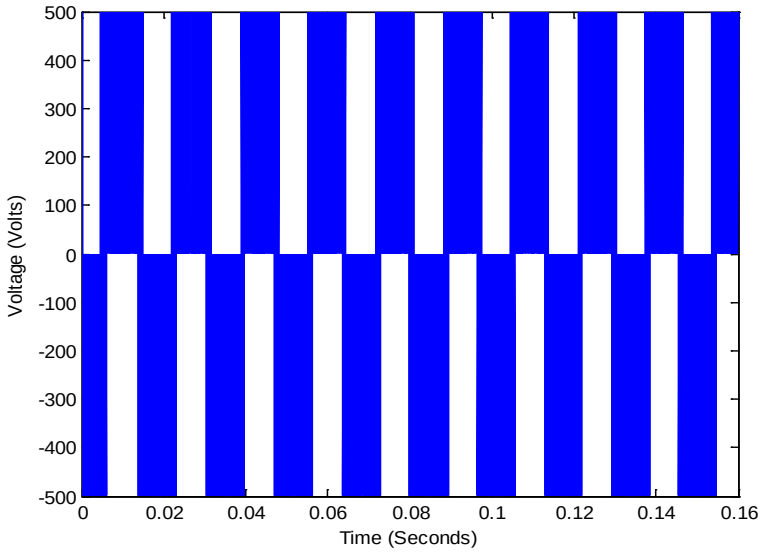

Figure 4-34: Voltage profile of inverter output if a single phase fault occurred at the secondary of the transformer T3 with 32KW PV generator connected to bus 7.

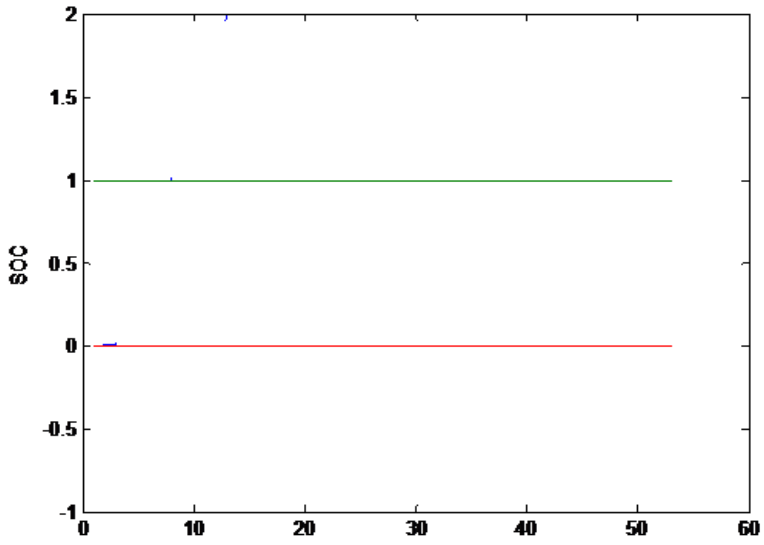

Figure 4-35: The ‘state of charge’ of the battery if a single phase fault occurs at the secondary of the transformer T3 with 32KW PV generator connected to bus 7

In figure 4.34 and 4.35 the output voltage of the inverter and battery's State of Charge are shown when the fault occurred at the secondary of the transformer T3 respectively.

CHAPTER 5

5.Conclusion

From the analysis of the results obtained above it is quite possible to conclude these points:

- With the integration of PV generator the voltage at the point of common coupling (PCC) increased.

- With the integration of the PV generator there are no harmonics produced this is because the capacity of the PV generator penetration is still low, but later if the capacity is increased this factor must be taken into consideration.

- Moreover with the increment in the capacity of the PV generator there are other problems associated with it which might arise they are: reactive power requirements, flicker, over-current protection practices, anti-islanding protection, and stress on the distribution transformer.

- The simulation using the Li-Ion battery model gives an ideal response of the system: the total time of battery charging (approximately seven hours). This is an excellent charging average, by taking into consideration that the amount of time that the same Li-Ion battery takes to fully charge using a DC power supplier is approximately three hours.

- In this thesis, over voltage at the point of common coupling (PCC) due to reverse power flow from PV generator and its solution with integrated battery control system have been studied with both steady-state and dynamic simulations of the developed model.

- Thus, it can be stated that the problem of the voltage rise at the point of common coupling can be minimized if the battery is programmed in a way that it will block the flow of power from Photovoltaic generator to the utility if the voltage at the PCC increased beyond the acceptable limit of voltage regulation.

5.1.Future Work

The following are the recommendations for advancing this work.

- The proposed design technique can be investigated for even larger systems.

- In addition to this, analysis can be done by placing two PV generators at two different locations.

- In this thesis, only single machine is considered analysis can be done by placing two machines or even more.

6.References

[1] V. Quaschning. Understanding Renewable Energy Systems. Earthscan Canada, 2005.

[2] Yuan-Kang Wu, Ching-Shan Chen, Yi-Shuo Huang, Ching-Yin Lee, “Advanced Analysis of Clustered Photovoltaic System’s Performance Based on the Battery-Integrated Voltage Control Algorithm”. International Journal of Emerging Electric Power Systems, Volume 10, Issue 4 2009 Article 3.

[3] Mohamed Azab, “Improved Circuit Model of Photovoltaic Array” Procedings of World Academy of Science, Engineering and Technology Volume 34 Ooctomer 2008 ISSN 2070-3740.

[4] Karen L. Butler-Purry, Matthew Marotti “Impact of Distributed Generators on Protective Devices in Radial Distribution Systems” IEEE, 2006.

[5] H. D. Young and R. A. Freedman. University Physics with Modern Physics. Pearson AddisonWesley, San Fransisco, CA, USA, 11th edition, 2004.

[6] Tyson Den Herder, “Design and Simulation of Photovoltaic Super System with Simulink”, Senior Project, California Polytechnic State University. 2006.

[7] M. A. Green. Solar Cells. Operating Principles, Technology and System Applications. The University of New South Wales, Kensington, NSW,Australia, 1998.

[8] Department of Physics C.R. Nave (Georgia State University and Astronomy). Hyperphysics, 2005. Retrieved October, 2007 from http://hyperphysics.phy-astr.gsu.edu/hbase/hframe.html.

[9] J. A. Gow, C. D. Manning “Development of a photovoltaic array model for use in power electronics simulation studies,” *IEE Proceedings on Electric Power Applications*, vol. 146, no. 2, pp. 193-200, March 1999.

[10] Francisco M. Gonzalez-Longatt, “Model of Photovoltaic Module in Matlab™”. 2 CIBILEC 2005.

[11] Huan-Liang Tsai, Ci-Siang Tu, and Yi-Jie Su, *Member*, IAENG, “Development of Generalized Photovoltaic Model Using MATLAB/SIMULINK” Proceedings of the

World Congress on Engineering and Computer Science 2008 WCECS 2008, October 22 - 24, 2008, San Francisco, USA.

[12] Anca D. Hansen, Poul Sorenson, Lars H. Hansen, Henrik Bindner, “Models for a Stand-Alone PV System”, Riso National Laboratory, Roskilde, 2000.

[13] Geoff Walker, “EVALUATING MPPT CONVERTER TOPOLOGIES USING A MATLAB PV MODEL”.

[14] R. Kiranmayi, K. Vijay Kumar Reddy, M. Vijay Kumar, “Modeling and a MPPT method for Solar Cells” Journal for Engineering and Applied Sciences, 3(1): 128-133, 2008.

[15] S.Chowdhury, S.P.Chowdhury, G.A.Taylor, Y.H.Song, “Mathematical Modelling and Performance Evaluation of a Stand-Alone Polycrystalline PV Plant with MPPT Facility”, IEEE, 2008.

[16] Carlos Manuel Ferriara Santos, “Optimized Photovoltaic Solar Charger With Voltage Maximum Power Point Tracking” 2008, Thesis Dissertation, Instituto Superior Tecnico, Universidade Technica de Lisboa.

[17] Gianfranco Chicco, Roberto Napoli, Filippo Spertino, “Performance Assessment of the Inverter-based Grid Connection of Photovoltaic Systems” ISSN 0005–1144, ATKAAF 45(3–4), 187–197 (2004).

[18] Johan H. R. Enslin, Peter J. M. Heskes, “Harmonic Interaction between a Large Number of Distributed Power Inverters and the Distribution Network”, IEEE Transactions on Power Electronics, VOL. 19, NO. 6, NOVEMBER 2004.

[19] B. Kroposki, R. DeBlasio, “Technologies for the New Millennium: Photovoltaics as a Distributed Resource” IEEE, March 2000.

[20] Benoit BLetterie, Michael Heidenreich, “Impact of large Photovoltaic penetration on the quality of the supply: A case study at a photovoltaic noise barrier in Austria”, 19th European Photovoltaic Solar Energy Conference and Exibition.

[21] Aldo Canova, Luca Giaccone, Filippo Spertino and Michele Tartaglia, “Electrical Impact Of Photovoltaic Plant In Distributed Network”.

[22] Alberto Parera Ruiz, Marcian Cirstea, Wlodzimierz Koczara, Remus Teodorescu, “A Novel Integrated Renewable Energy System Modelling Approach, Allowing Fast FPGA Controller Prototyping”.

[23] Salvatore Favuzza, Filippo Spertino, Giorgio Graditi, Gianpaolo Wale, “Comparison of Power Quality Impact of Different Photovoltaic Inverters: the viewpoint of the grid”, 2004 IEEE International Conference on Industrial Technology (KIT).

[24] Adly Girgis, Sukumar Brahma, “Effect of Distributed Generation on Protective Device Coordination in Distribution System” IEEE, 2001.

[25] Yuzuru Ueda, Kosuke Kurokawa, Member, IEEE, Takayuki Tanabe, Kiyoyuki Kitamura, and Hiroyuki Sugihara, “Analysis Results of Output Power Loss Due to the Grid Voltage Rise in Grid-Connected Photovoltaic Power Generation Systems” IEEE TRANSACTIONS ON INDUSTRIAL ELECTRONICS, VOL. 55, NO. 7, JULY 2008.

[26] Y.Ueda, T.Oozeki, K.Kurokawa, T.Itou, K.Kitamura, Y.Miyamoto, M.Yokota, H.Sugihara, S.Nishikawa, “DETAILED PERFORMANCE ANALYSES RESULTS OF GRID-CONNECTED CLUSTERED PV SYSTEMS IN JAPAN –FIRST 200 SYSTEMS RESULTS OF DEMONSTRATIVE RESEARCH ON CLUSTERED PV SYSTEMS”,

[27] [Mann04] – Mann Kin (Eddie) Lee, Implementation of Photovoltaic Maximum Power Tracking using a Microcontroller, Ph. D. Thesis, Curtin University of Technology, Curtin, September 2004.

Annexure 1

SUNTECH

Solar powering a green future™

BLACK LABEL™ STP180S - 24/Ac
STP175S - 24/Ac
STP170S - 24/Ac

Electrical Characteristics

Characteristics	STP180S-24/Ac	STP175S-24/Ac	STP170S-24/Ac
Open - Circuit Voltage (Voc)	44.8V	44.7V	44.4V
Optimum Operating Voltage (Vmp)	36.0V	35.8V	35.6V
Short - Circuit Current (Isc)	5.29A	5.23A	5.15A
Optimum Operating Current (Imp)	5.0A	4.9A	4.8A
Maximum Power at STC (Pmax)	180Wp	175Wp	170Wp
Operating Temperature	-40°C to +85°C	-40°C to +85°C	-40°C to +85°C
Maximum System Voltage	1000V DC	1000V DC	1000V DC
Maximum Series Fuse Rating	8A	8A	8A
Power Tolerance	±3 %	±3 %	±3 %

STC: Irradiance 1000W/m², Module temperature 25°C, AM=1.5

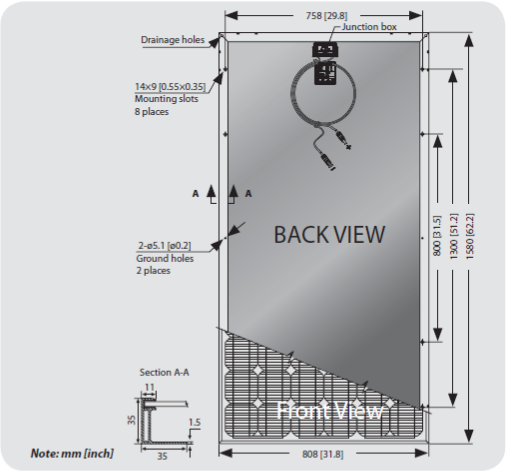

Mechanical Characteristics

Solar Cell	Mono-crystalline 125×125mm (5inch)
No. of Cells	72 (6×12)
Dimensions	1580×808×35mm (62.2×31.8×1.4inch)
Weight	15.5kg (34.1lbs.)
Front Glass	3.2 mm (0.13inch) tempered glass
Frame	Anodized aluminium alloy
Junction Box	IP65 rated
Output Cables	LAPP 4.0mm²(0.006inch²), asymmetrical lengths (-) 1200mm(47.2inch) and (+)800mm(31.5inch), MC Plug Type IV connectors

Temperature Coefficients

Nominal Operating Cell Temperature (**NOCT**)	45±2°C
Temperature Coefficient of Pmax	-0.48 %/°C
Temperature Coefficient of Voc	-0.34 %/°C
Temperature Coefficient of Isc	0.037 %/°C

Current-Voltage & Power-Voltage Curve (175W)

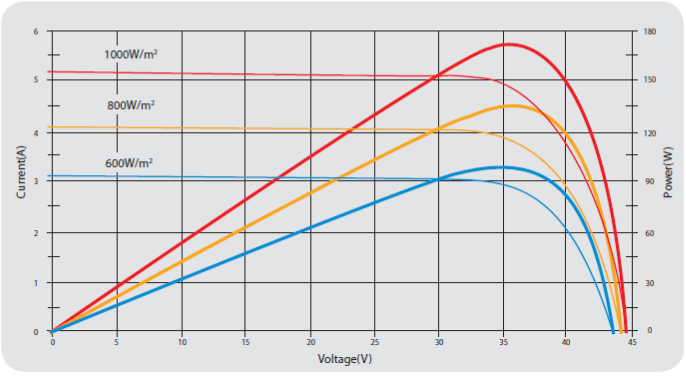

Temperature Dependence of Isc, Voc, Pmax

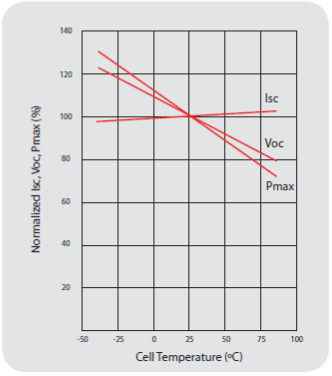

Specifications are subjected to change without further notice

Vita

Name: Mir Shahed Ali

Date of Birth: 22nd April 1983

Nationality: Indian

Bachelor Degree: Bachelor of Engineering in Electrical & Electronics from Osmania University (2005), Hyderabad, A.P., INDIA.

Masters Degree: Master of Science in Electrical Engineering (December 2010), from King Fahd University of Petroleum & Minerals, Dhahran, Saudi Arabia.

Present Address: Bldg. No. 811, Room No. 216,

King Fahd University of Petroleum & Minerals,

KFUPM Box 8337,

Dhahran 31261, Saudi Arabia.

Permanent Address: H.No: 20-1-350/E,

Koka Bazar, Hussaini Alam,

Serial No. 263

Hyderabad-64,

A.P., INDIA.

Contact No. +966 55 8503209

+91 9246595107, +91 9177480164.

Email Id: shahedalii@yahoo.com, mirshahedali4@gmail.com